High net CO_2 and CH_4 release at a eutrophic shallow lake on a formerly drained fen

D. Franz[1], F. Koebsch[1], E. Larmanou[1], J. Augustin[2] and T. Sachs[1]

[1] {Helmholtz Centre Potsdam, GFZ German Research Centre for Geosciences, Telegrafenberg, 14473 Potsdam, Germany}

[2] {Institute for Landscape Biogeochemistry, Leibniz Centre for Agricultural Landscape Research (ZALF), Eberswalder Str. 84, 15374 Müncheberg, Germany}

Correspondence to: D. Franz (daniela.franz@gfz-potsdam.de)

Abstract

Drained peatlands often act as carbon dioxide (CO_2) hotspots. Raising the groundwater table is expected to reduce their CO_2 contribution to the atmosphere and revitalize their function as carbon (C) sink in the long term. Without strict water management rewetting often results in partial flooding and the formation of spatially heterogeneous, nutrient-rich shallow lakes. Uncertainties remain as to when the intended effect of rewetting is achieved, as this specific ecosystem type has hardly been investigated in terms of greenhouse gas (GHG) exchange. In most cases of rewetting, methane (CH_4) emissions increase under anoxic conditions due to a higher water table and in terms of global warming potential (GWP) outperform the shift towards CO_2 uptake, at least in the short-term.

Based on eddy covariance measurements we studied the ecosystem–atmosphere exchange of CH_4 and CO_2 at a shallow lake situated on a former fen grassland in Northeast (NE) Germany. The lake evolved shortly after flooding, 9 years previous to our investigation period. The ecosystem consists of two main surface types: open water (inhabited by submerged and floating vegetation) and emergent vegetation (particularly including the eulittoral zone of the lake, dominated by *Typha latifolia*). To determine the individual contribution of the two main surface types to the net CO_2 and CH_4 exchange of the whole lake ecosystem, we combined footprint analysis with CH_4 modelling and net ecosystem exchange (NEE) partitioning.

The CH_4 and CO_2 dynamics were strikingly different between open water and emergent vegetation. Net CH_4 emissions from the open water area were around 4-fold higher than from emergent vegetation stands, accounting for 53 and 13 g CH_4 m^{-2} a^{-1}, respectively. In addition, both surface types were net CO_2 sources with 158 and 750 g CO_2 m^{-2} a^{-1}, respectively. Unusual meteorological conditions in terms

of a warm and dry summer and a mild winter might have facilitated high respiration rates. In sum, even after 9 years of rewetting the lake ecosystem exhibited a considerable C loss and global warming impact, the latter mainly driven by high CH_4 emissions. We assume the eutrophic conditions in combination with permanent high inundation as major reasons for the unfavourable GHG balance.

1 Introduction

Peatland ecosystems play an important role in global greenhouse gas (GHG) cycles, although they cover only about 3 % of the earth´s surface (Frolking et al. 2011). Peat growth depends on the proportion of carbon (C) sequestration and release. Pristine peatlands act as long-term C sinks and are near-neutral (slightly cooling) regarding their global warming potential (GWP; Frolking et al. 2011), dependent on rates of C sequestration and methane (CH_4) emissions. However, many peatlands worldwide are used e.g. for agriculture, as are more than 85% of the peatlands in Germany and the Netherlands (Silvius et al. 2008). Drainage is associated with shrinkage and internal phosphor fertilisation of the peat (Zak et al. 2008). Moreover, the hydrology of the area as well as physical and chemical peat characteristics are changing (Holden et al. 2004, Zak et al. 2008). Above all, drained and intensively managed peatlands are known as strong sources of carbon dioxide (CO_2; e.g. Joosten et al. 2010, Hatala et al. 2012, Beetz et al. 2013). On the other hand, lowering the water table is typically accompanied with decreasing CH_4 emissions (Roulet et al. 1993). Emission factors of 1.6 g CH_4 m^{-2} a^{-1} and 2235 g CO_2 m^{-2} a^{-1} were assigned to temperate deep-drained nutrient-rich grassland in the 2013 wetland supplement to the 2006 IPCC Guidelines for National Greenhouse Gas Inventories (IPCC 2014).

In the last decades rewetting of peatlands attracted attention in order to stop soil degradation, reduce CO_2 emissions and to recover their functions as C and nutrient sink and ecological habitat (Zak et al. 2015). Large rewetting projects were initiated, e.g. the Mire Restoration Program of the federal state of Mecklenburg-West Pomerania in Northeast (NE) Germany (Berg et al. 2000) starting in 2000 and involving 20 000 ha of formerly drained peatlands, thereby especially fens (Zerbe et al. 2013) e.g. in the Peene river catchment. However, uncertainties remain as to when the intended effects of rewetting are achieved. Only few studies exist on the temporal development of GHG emissions of rewetted fens, especially on longer time scales. Augustin and Joosten (2007) discuss three very different states following peatland rewetting based on observations at Belarusian mires, though without specifying the individual lengths of the phases. Broad agreement exists concerning the CH_4 hot spot characteristic of newly rewetted peatlands (e.g. Meyer et al. 2001, Hahn-Schöfl et al. 2011, Knox et al. 2015). However, a rapid recovery of the net CO_2 sink function is not consistently reported (e.g. Wilson et al. 2007).

Peatlands develop a distinct microtopography after drainage and subsequent subsidence. Rewetting e.g. in the Peene river catchment resulted in the formation of large-scale shallow lakes in the lower parts of the fens, with water depths usually below 1 m (Zak et al. 2015, Steffenhagen et al. 2012). These new ecosystems are nutrient-rich and most often strikingly different from natural peatlands. They experience a rapid secondary plant succession (Zak et al. 2015). Helophytes are expected to progressively enter the open water body over the time leading to the terrestrialisation of the shallow lake and in the best case peat formation. However, this new ecosystem type and its progressive transformation have hardly been investigated in terms of GHG dynamics. The ecosystem-inherent spatial heterogeneity suggests complex patterns of GHG emissions due to distinct GHG source or sink characteristics of the involved surface types (generally open water and the littoral zone) resulting in measurement challenges. Site-specific heterogeneity implicitly has to be considered for the evaluation of ecosystem scale flux measurements (e.g. Barcza et al. 2009, Hendriks et al. 2010, Herbst et al. 2011, Hatala Matthes et al. 2014). The importance of small open water bodies in wetlands as considerable GHG sources was highlighted in previous studies (e.g. by Schrier-Uijl et al. 2011, Zhu et al. 2012, IPCC 2014) and in case of CH_4 even for landscape-scale budgets e.g. by Repo et al. (2007). In addition, the littoral zone of lakes is often found to be a CH_4 hot spot (Juutinen et al. 2003, Wang et al. 2006) with a contribution of up to 90 % to the whole-lake CH_4 release (Smith and Lewis 1992), albeit depending on the lake size (Bastviken et al. 2004) and plant community. Rõõm et al. (2014) measured the largest CH_4 (and CO_2) emissions of a temperate eutrophic lake at the helophyte zone within the littoral.

The objectives of this study are 1) to investigate the ecosystem-atmosphere exchange of CH_4 and CO_2 (NEE) of a nutrient-rich lake ecosystem emerged at a former fen grassland and 2) particularly infer the individual GHG dynamics of the main surface types within the ecosystem and quantify their contribution to the annual exchange rates. Therefore, we applied the eddy covariance technique from May 2013 to May 2014 and used an analytical footprint model to downscale the spatially integrated, half-hourly fluxes to the main surface types “open water” and “emergent vegetation”. The resulting source area (i.e. spatial origin of the flux) fractions were then included in a temperature response (CH_4) and NEE partitioning model (CO_2) in order to quantify the source strength of the two surface types.

2 Material and methods

2.1 Study site

The study site “Polder Zarnekow” is a rewetted, rich fen (minerotrophic peatland) located in the Peene river valley (Mecklenburg-West Pomerania, NE Germany, 53°52.5’ N 12°53.3’ E, see Fig. 1), with less than 0.5 m a.s.l. elevation. It is part of the Terrestrial Environmental Observatories Network (TERENO).

The temperate climate is characterised by a long-term mean annual air temperature and mean annual precipitation of 8.7 °C and 584 mm, respectively (German Weather Service, meteorological station Teterow, 24 km SW of the study site; reference period 1981–2010). The geomorphological character of the area is predominantly a result of the Weichselian glaciation as the last period of the Pleistocene (Steffenhagen et al. 2012). The fen developed with continuous percolating groundwater flow (Succow 2001). Peat depth partially reaches 10 m (Hahn-Schöfl et al. 2011). Drainage was initialized in the 18th century and strongly intensified between 1960 and 1990 within an extensive melioration program (Höper et al. 2008). The decline of the water table to > 1 m below surface and subsequent decomposition and mineralisation of the peat (especially in the upper 30 cm, Hahn-Schöfl et al. 2011) caused phosphor fertilisation (Zak et al. 2008) and soil subsidence to levels below that of adjacent freshwater bodies (Steffenhagen et al. 2012, Zerbe et al. 2013). The latter simplified the rewetting process which was initiated in winter 2004/2005 by opening the dikes.

In consequence of flooding the drained fen was converted into a spatially heterogeneous site of emergent vegetation (on temporarily inundated soil) and permanent open water areas. In this study we focus on a eutrophic and polymictic lake (open water body about 7.5 ha) as part of the rewetted area, with water depths ranging from 0.2 to 1.2 m (2004 to 2012; Zak et al. 2015). During the study period the open water body of the lake was inhabited by submerged and floating macrophytes, particularly *Ceratophyllum demersum*, *Lemna minor*, *Spirodela polyrhiza* (Steffenhagen et al. 2012) and *Polygonum amphibium*, which rather corresponds to the sublittoral zone in a typical lake zonation. *Ceratophyllum* and *Lemna* sp. were already reported to colonise the lake in the second year of rewetting (Hahn-Schöfl et al. 2011). *Phalaris arundinacea*, that dominated the fen before rewetting, died off in the first year of inundation (Hahn-Schöfl et al. 2011) and has been limited to the non-inundated periphery of the ecosystem. Helophytes (e.g. *Glyceria*, *Typha*) started the colonisation of lake margins and other temporarily inundated areas in the third year of rewetting. The eulittoral zone of the lake is now dominated by *Typha latifolia* stands gradually colonising the open water in the last years. Emergent vegetation stands also include sedges as *Carex gracilis* (Steffenhagen et al. 2012). At the bottom of the shallow lake an up to 30 cm thick layer of organic sediment evolved, initially fed by fresh plant material of the former vegetation and since then continuously replenished by recent aquatic plants and helophytes after die-back (Hahn-Schöfl et al. 2011).

2.2 Eddy covariance and additional measurements

We conducted eddy covariance (EC) measurements of CO_2 and CH_4 exchange on a tower placed on a stationary platform at the NE edge of the shallow lake (see Fig. 1). Thereby we ensured to frequently catch the signal from both the open water body and the *Typha latifolia* dominated belt of the shallow lake (eulittoral zone). We defined an area of interest (AOI) in order to focus on an ecosystem

dominated by a shallow lake and to avoid a possible impact of the farm and grassland to the north of the shallow lake. The EC measurement setup included: an ultrasonic anemometer for the 3D wind vector (*u*, *v*, *w*) and sonic temperature (HS-50, Gill, Lymington, Hampshire, UK), an enclosed-path infrared gas analyser (IRGA) and an open-path IRGA for CO_2/H_2O and CH_4 concentrations, respectively (LI-7200 and LI-7700, LI-COR Biogeosciences, Lincoln NE, USA). Flowrate was about 10-11 l min^{-1}. Measurement height was on average 2.63 m above the water surface at the position of the tower, depending on the water level. We recorded raw turbulence and concentration data with a LI-7550 digital data logger system (LI-COR Biogeosciences, Lincoln NE, USA) at 20 Hz in half-hourly files. The dataset is shown in Coordinated Universal Time (UTC), which is 1 hour behind local time (LT).

We further equipped the tower with instrumentation for net radiation, air temperature/humidity, 2D wind direction and speed, incoming and reflected photosynthetic photon flux density (PPFD/PPFDr) and water level. Additional measurements in close proximity to the tower included precipitation, soil heat flux as well as soil and water temperature. Soil temperature was measured below the water column in depths of 10 cm, 20 cm, 30 cm, 40 cm and 50 cm and water temperature at the sediment-water-interface. All non-eddy covariance-related measurements were logged as 1 min averages/sums (precipitation). Gaps were filled with measurements of the Leibniz Centre for Agricultural Landscape Research (ZALF, Müncheberg, Germany) at the same platform and a nearby climate station (Climate station Karlshof, GFZ German Research Centre for Geosciences, 14 km distance from study site, Itzerott 2015).

A water density gradient was calculated based on the temperature at the water surface and at the sediment-water interface. The water surface temperature was calculated based on the Stefan-Boltzmann law:

$$T_w = \sqrt[4]{\frac{I}{\varepsilon_w \, \sigma_{SB}}} \quad (1)$$

where T_w is the water surface temperature (K), I is the long-wave outgoing radiation (W m^{-2}), ε_w is the infrared emissivity of water (0.960) and σ_{SB} is the Stefan–Boltzmann constant ($5.67 \cdot 10^{-8}$ W m^{-2} K^{-4}). We calculated the density of the air-saturated water at the water surface and the sediment-water interface according to Bignell (1983):

$$\rho_{as} = \rho_{af} - 0.004612 + 0.000106 * T \quad (2)$$

where ρ_{as} is the density of the respective air-saturated water (k m^{-3}), ρ_{af} is the density of the respective air-free water (k m^{-3}; see Wagner and Pruß 2002) at atmospheric pressure (1013 hPa) and T is the respective water temperature (°C). The gradient of the two water densities (air-saturated)

$\Delta\rho/\Delta z$ was calculated as difference of the water density (air-saturated) at the sediment-water interface and the surface water density (air-saturated), divided by the distance (m) between the two basic temperature measurements. Changes of the distance due to the fluctuating water level were considered. Positive and negative gradients indicate periods of stratification and thermally induced convective mixing of the water column, respectively.

2.3 Flux computation and further processing

For this analysis we used data from 14 May 2013 to 14 May 2014. We calculated half-hourly fluxes of CO_2 and CH_4 based on the covariances between the respective scalar concentration and the vertical wind velocity using the processing package EddyPro 5.2.0 (LI-COR, Lincoln, Nebraska, USA). Sonic temperature was corrected for humidity effects according to van Dijk et al. (2004). Artificial data spikes were removed from the 20 Hz data following Vickers and Mahrt (1997). We used the planar fit method (Finnigan et al. 2003, Wilczak et al. 2001) for axis rotation and defined the sector borders according to Siebicke et al. (2012). Block averaging was used to detrend turbulent fluctuations. For time lag compensation we applied covariance maximization (Fan et al. 1990). Spectral losses due to crosswind and vertical instrument separation were corrected according to Horst and Lenschow (2009). The methods of Moncrieff et al. (2004) and Fratini et al. (2012) were used for the correction of high-pass filtering and low-pass filtering effects, respectively. For fluctuations of CH_4 density we corrected changes in air density according to Webb et al. (1980), considering LI-7700-specific spectroscopic effects (McDermitt et al. 2011). According to the micrometeorological sign convention, positive values represent fluxes from the ecosystem into the atmosphere (emission) and negative values fluxes from the atmosphere into the ecosystem (ecosystem uptake).

2.4 Quality assurance

We filtered the averaged fluxes according to their quality as follows (see Table 1, for final measurement data coverage see Fig. A1):

- We rejected fluxes with quality flag 2 (QC 2, bad quality) based on the 0-1-2 system of Mauder and Foken (2004).
- CH_4 fluxes were skipped if the signal strength (RSSI) was below the threshold of 14 %. This threshold was estimated according to Dengel et al. (2011).
- Fluxes with friction velocity (u*) < 0.12 m s^{-1} and > 0.76 m s^{-1} were not included due to considerably high fluxes beyond these thresholds, which were estimated similar to the procedure described in Aubinet et al. (2012) based on binned u* classes. The storage term was calculated as described in Béziat et al. (2009).

- Unreasonably high positive and negative fluxes (0.2 %/99.8 % percentile) were discarded from the CO_2 and CH_4 flux dataset.

Quality control (apart from EddyPro internal steps) and the subsequent processing steps were performed with the free software environment R (R Core Team 2012).

2.5 Footprint modelling

We applied footprint analysis to determine the source area including the fractions of the surface types of each quality-controlled half-hourly flux using a footprint calculation procedure following Göckede et al. (2004). The source area functions were calculated based on the analytical footprint model of Kormann and Meixner (2001). Roughness length and vegetation height were estimated with an iterative algorithm (see also Barcza et al. 2009). Based on an aerial image (GoogleEarth, http://earth.google.com/) the surface of our study site was classified into two main types and implemented in a land cover grid: "open water" including in particular the open water body of the shallow lake and "emergent vegetation" with a height up to 2 m and including the eulittoral zone of the shallow lake dominated by *Typha latifolia*. The cumulative annual footprint climatology was calculated following Chen et al. (2011). Fluxes were excluded where footprint information was not available or more than 20 % of the source area was outside the AOI (see Fig. 1 and Table 1). The fractional coverage within the AOI (A_i) was 21.7 % for open water.

Quasi-continuous source area information for the two surface types were achieved by gapfilling the results of the footprint model with the means of the source area fractions of the surface types (Ω_i) for 1°-wind direction-intervals, separately for stable and unstable conditions. In case the sum of the Ω_i was less than 100 %, when the source area exceeded the set borders, we assigned the remaining contribution percentages to emergent vegetation, as the area beyond the borders is dominated by emergent vegetation rather than open water.

2.6 Gapfilling

A Marginal Distribution Sampling (MDS)) approach proposed by Reichstein et al. (2005), available as web tool based on the R package REddyProc (http://www.bgc-jena.mpg.de/REddyProc/brew/REddyProc.rhtml) was applied for gapfilling and partitioning of NEE measurements ($MDS_{CO2nofoot}$), with air temperature as temperature variable. For the gapfilling of CH_4 measurements non-linear regression (NLR) was applied ($NLR_{CH4nofoot}$):

$$F_{CH_4} = \exp(a + b_1 \cdot X_1 + \ldots + b_j \cdot X_j) \quad (3)$$

where a and $b_1 \ldots b_j$ are fitting parameters and $X_1 \ldots X_j$ are environmental parameters. Several environmental parameters, which were reported to be correlated with CH_4 flux on different time scales, were tested to find the best bi- or multivariate NLR model for the ecosystem CH_4 flux: pressure change, u*, PAR, air temperature, soil heat flux, soil/peat temperature in different heights and waterlevel. Only fluxes of the best quality (QC 0) were used to fit the NLR model and the MDS.

2.7 Calculation of the annual CO_2 and CH_4 budget and the global warming potential (GWP)

We used the continuous flux datasets derived from gapfilling for the calculation of annual CO_2 and CH_4 budgets. The ecosystem GHG balance was calculated by summation of the net ecosystem exchange of CO_2 and CH_4 using the global warming potential (GWP) of each gas at the 100-year time horizon (IPCC, 2013). According to the IPCC AR5 (IPCC, 2013) CH_4 has a 28-fold global warming potential compared to CO_2 (without inclusion of climate-carbon feedbacks).

The uncertainty of the annual estimates was calculated as the square root of the sum of the squared random error (measurement uncertainty) and gapfilling error within the one-year observation period (see e.g. Hommeltenberg et al. 2014, Shoemaker et al. 2015). An estimation of the random uncertainty due to the stochastic nature of turbulent sampling according to Finkelstein and Sims (2001) is implemented in EddyPro 5.2.0. In case of the MDS approach the gapfilling error (standard error) was calculated from the standard deviation of the fluxes used for gapfilling, provided by the web tool. For budgets based on the NLR approach we used the residual standard error of the NLR model as gapfilling error (following Shoemaker et al. 2001).

2.8 Estimation of surface type fluxes

To estimate the specific surface type fluxes, we combined footprint analysis with NEE partitioning (using NLR) to assign gross primary production (GPP) and ecosystem respiration (R_{eco}) to the two main surface types ($NLR_{CO2foot}$). R_{eco} and GPP were modelled as sum of the two surface type fluxes weighted by Ω_i (analogous to Forbrich et al. 2011). Night-time R_{eco} (global radiation < 10 W m^{-2}) was estimated by the exponential temperature response model of Lloyd and Taylor (1994) assuming that night-time NEE represents the night-time R_{eco}:

$$R_{eco} = \sum_{i=1}^{2} \Omega_i \cdot R_{ref_i} \cdot \exp\left(E_{0_i}\left(\frac{1}{T_{ref} - T_0} - \frac{1}{T_{air} - T_0}\right)\right) \quad (4)$$

where R_{eco} is the half-hourly measured ecosystem respiration (µmol^{-1}m^{-2}s^{-1}), Ω_i is the source area fraction of the respective surface type, R_{ref} is the respiration rate at the reference temperature T_{ref} (283.15 K), E_0 defines the temperature sensitivity, T_0 is the starting temperature constant (227.13 K)

and T_{air} the mean air temperature during the flux measurement. The model parameters achieved for night-time R_{eco} were applied for the modelling of day-time R_{eco}. GPP was calculated by subtracting day-time R_{eco} from the measured NEE. GPP was further modelled using a rectangular, hyperbolic light response equation based on the Michaelis–Menten kinetic (see e.g. Falge et al. 2001):

$$GPP = \sum_{i=1}^{2} \Omega_i \cdot \left(\frac{GP_{max_i} \cdot \alpha_i \cdot PAR}{\alpha_i \cdot PAR + GP_{max_i}}\right) \quad (5)$$

where GPP is the calculated gross primary production ($\mu mol^{-1} m^{-2} s^{-1}$), Ω_i is the source area fraction of the respective surface type, GP_{max} is the maximum C fixation rate at infinite photon flux density of the photosynthetic active radiation PAR ($\mu mol^{-1} m^{-2} s^{-1}$), α is the light use efficiency (mol CO_2 mol^{-1} photons). We calculated one parameter set for R_{eco} and GPP per day based on a moving window of 28 days. In order to avoid over-parameterization we introduced fixed values of 150 for E_0 and -0.03 and -0.01 for α of emergent vegetation and water bodies, respectively, to get reasonable parameter values for R_{ref} and GP_{max}. We excluded parameter sets for R_{eco} or GPP, if one of the two R_{ref} and GP_{max} parameter values was insignificant (p-value ≥ 0.05), negative or zero. In addition, the 1 %/99 % percentiles of GP_{max} were excluded. These gaps within the parameter set were filled by linear interpolation. Gaps remained in R_{eco} and GPP time series due to gaps in the environmental variables. Gaps up to 3 hours length were filled by linear interpolation. Larger gaps were filled with the mean of the flux during the same time of the day before and after the gap. Due to the moving window approach, we could not estimate model parameters for the first and last 14 days of our study period. Instead, we applied the first and last estimated parameter set, respectively. Modelled GPP and R_{eco} were summed up to half-hourly NEE fluxes and used for alternative NEE gapfilling ($NLR_{CO2foot}$).

As for NEE we expect different CH_4 emission rates of the two surface types. Thus, we extended the NLR model ($NLR_{CH4nofoot}$) in a way that the CH_4 flux is the sum of the two surface type fluxes weighted by Ω_i ($NLR_{CH4foot}$):

$$F_{CH_4} = \sum_{i=1}^{2} \Omega_i \cdot \exp(a_i + b_{1i} \cdot X_1 + \ldots + b_{ji} \cdot X_j) \quad (6)$$

where Ω_1 is the source area fraction of the respective surface type. Considering the principle of parsimony, we combined up to three parameters besides the contribution of the surface types. Remaining gaps were filled by interpolation. Surface type CO_2 and CH_4 fluxes were derived based on the fitted NLR parameters.

We calculated the annual budgets of CO_2 and CH_4 for the EC source area, the surface types (assuming source area fraction of 100 % for the respective surface type) and the AOI, the latter following Forbrich et al. (2011) by applying Eq. 4 and Eq. 5 for CO_2 as well as Eq. 6 for CH_4 with the fitted parameters, but

A_i instead of Ω_i as weighting surface type contribution. The gapfilling error for the $NLR_{CO2foot}$ model was based on the residual standard error of both R_{eco} and GPP.

3 Results

3.1 Environmental conditions and fluxes of CO_2 and CH_4

Mean annual air temperature and annual precipitation for the study period were 10.1 °C and 416.5 mm, respectively, indicating an unusual dry and warm measurement period compared to the long-term average. The summer 2013 was among the 10 warmest since the beginning of the measurements in 1881 (German Weather Service DWD). From June to August monthly averaged air temperature was 0.2 up to 0.9 °C higher and precipitation was 9.1 up to 38.1 mm less than the long-term averages. The open water area of the shallow lake was densely vegetated with submerged and floating macrophytes. A summertime algae slick accumulated in the NE part of the shallow lake. Winter 2013/2014 was characterised by exceptionally mild temperatures and very sparse precipitation. However, a short cold period (see Fig. 2) resulted in ice cover on the shallow lake between 21 January and 16 February 2014. The water level of the shallow lake fluctuated between 0.36 and 0.77 m (at the position of the sensor) and had its minimum at the end of August/beginning of September and its maximum in January. We observed the exposure of normally inundated soil surface at emergent vegetation stands during the dry period in summer 2013.

Both CO_2 and CH_4 flux measurement time series showed a clear seasonal trend with a median CO_2 flux of 0.57 μmol m^{-2} s^{-1} and a median CH_4 flux of 0.02 μmol m^{-2} s^{-1}. CH_4 emissions peaked in mid-August 2013 with 0.57 μmol m^{-2} s^{-1}. The highest net CO_2 uptake (-15.34 μmol m^{-2} s^{-1}) and release (21.04 μmol m^{-2} s^{-1}) were both observed in June 2013. To investigate the potential presence of a diurnal cycle of CO_2 and CH_4 fluxes throughout the study period we normalised the mean half-hourly CO_2 and CH_4 fluxes per month with the respective minimum/ maximum and median of the half-hourly fluxes of the specific month (modified from Rinne et al. 2007). A pronounced diurnal cycle of CO_2 fluxes with peak uptake around midday and peak release around midnight was obvious until November 2013 and beginning in March 2014 (see Fig. 3), although less pronounced in these two months. We found a clear diurnal cycle of CH_4 fluxes from June to September 2013 and in March 2014 (April 2014 based on 3 days only and May 2014 not available as the sensor was dismantled) with daily peaks during night-time (around midnight until early morning). The water density gradient indicates thermally induced convective mixing of the whole water column at the same time of the day from May until October 2013 and from February to May 2014. In May 2014 the diurnal pattern of the water density gradient was less pronounced than in May 2013.

3.2 Gapfilling performance and annual budgeting of CO_2, CH_4, C and GWP

The $MDS_{CO2nofoot}$ approach explained 74 % of the variance in NEE (see Table 2). Median NEE accounted for 1.9 g CO_2 m^{-2} d^{-1}. The annual budget of gapfilled NEE ($MDS_{CO2nofoot}$) between 14 May 2013 and 14 May 2014 was 524.5 ± 5.6 g CO_2 m^{-2} (see Table 3), characterising the site as strong CO_2 source with moderate rates of R_{eco} and GPP. We found a surprising CO_2 release strength during summer 2013, where already at the end of June daily R_{eco} often exceeded GPP. The highest daily CO_2 emission and uptake rates of 24.8 g CO_2 m^{-2} d^{-1} and -27.9 g CO_2 m^{-2} d^{-1} were both revealed in the beginning of July 2013 (see Fig. 2). July 2013 accounted for 23.2 % and 25.8 % of the annual R_{eco} and GPP, respectively. In addition, net CO_2 release outside the growing season (definition of the growing season following Lund et al. 2010; until 19 November 2013 and starting 26 February 2014) was 203.7 g CO_2 m^{-2} with a median of 2.2 g CO_2 m^{-2} d^{-1}.

The environmental variable giving the best NLR model for CH_4 was soil temperature in 10 cm depth (T_{s10}):

$$F_{CH_4} = \exp(-7.224 + 0.313 \cdot T_{s10}) \quad (7)$$

The model described 79 % of the variance in CH_4 flux (see Table 2). Including additional environmental variables to the regression function did not increase the model performance significantly. Cumulative CH_4 emissions were 40.5 ± 0.2 g CH_4 m^{-2} a^{-1} (see Table 3). Median CH_4 emissions were 41.9 mg m^{-2} d^{-1}, peaked at the end of July 2013 with 0.6415 g CH_4 m^{-2} d^{-1} and were at the minimum in January 2014 (see Fig. 2). The month with the highest proportion of annual CH_4 emissions was August 2013 (27.3 %). Non-growing season CH_4 fluxes only accounted for a small proportion within the annual budget, about 0.8 g CH_4 m^{-2}.

The site was an effective C and GHG source, accounting for 173.4 ± 1.7 g C m^{-2} a^{-1} and 1658.5 ± 11.2 g CO_2-Eq. m^{-2} a^{-1} for the EC source area (see Fig. 4). The proportion of CO_2 in the C and GWP budget was 82.5 % and 31.6 %, respectively. Components of the annual net C balance other than CO_2 and CH_4 fluxes, e.g. dissolved C, are not considered in this study. Our uncertainty estimates are within the range of similar studies (e.g. Shoemaker et al. 2015).

3.3 Source area composition and spatial heterogeneity of CO_2 and CH_4 exchange

Footprint analysis revealed the peak contribution in an average distance of 18 m from the tower and mainly from the open water area of the shallow lake (see Fig. 5). Open water covered on average 62.5 % of the EC source area. The two surface types showed different emission rates in terms of higher CH_4 fluxes and lower NEE rates with increasing Ω_{water} (see Fig. 6). Within the $NLR_{CO2foot}$ approach both

surface types were denoted as sources of CO_2, but with about 4-fold stronger rates of GPP, R_{eco} and NEE for emergent vegetation compared to open water (see Fig. 7 and Table 3). The approach yielded a similar cumulative annual NEE for the whole EC source area including both surface types as the $MDS_{CO2nofoot}$ approach, but lower component fluxes (GPP and R_{eco}). As for CO_2, we implemented Ω_i as weighting factors within the NLR model for CH_4 ($NLR_{CH4foot}$) to get the surface type specific fluxes of CH_4 and fitted the parameters as follows:

$$F_{CH_4} = \Omega_{veg} \cdot \exp(-10.076 + 0.415 \cdot T_{s10}) + \Omega_{water} \cdot \exp(-6.449 + 0.286 \cdot T_{s10}) \quad (8)$$

Open water accounted for more than 4-fold higher emissions than the vegetated areas (see Fig. 7 and Table 3). The $NLR_{CH4foot}$ approach revealed a similar annual CH_4 budget as the $NLR_{CH4nofoot}$ approach.

Annual budgets of CO_2 (844 g CO_2 m^{-2} a^{-1}) and CH_4 (22 g CH_4 m^{-2} a^{-1}) for the AOI differed strongly from the budgets for the EC source area due to the contrasting emission rates of open water and emergent vegetation (see Table 3) and different fractional coverages of the surface types within the AOI and the EC source area. This resulted in a higher C loss (246.5 g C m^{-2} a^{-1}) and a lower GWP (1452.9 g CO_2-Eq. m^{-2} a^{-1}) for the AOI than for the EC source area. In the following we will primarily discuss the budgets of the EC source area and the surface types.

4 Discussion

4.1 Diurnal variability of CH_4 emissions

In terms of its daily cycle, CH_4 exchange between wetland ecosystems and the atmosphere is not generalisable, but rather dependent on the spatial characteristics of the wetland and thus, the impact of the individual CH_4 emission pathways (diffusion, ebullition, plant-mediated transport). Our measurements showed a diurnal cycle of CH_4 exchange from June to September 2013 and in March 2014, with the strongest emissions during night, as reported for shallow lakes (e.g. Podgrasjek et al. 2014) and wetland sites with a considerable fraction of open water (e.g. Godwin et al. 2013). In comparison, wetland CH_4 emissions were also reported to show daily maxima at day-time (e.g. Morrisey et al. 1993, Hendriks et al. 2010, Hatala Matthes et al. 2014), especially at sites with high abundance of vascular plants. No diurnal pattern (e.g. Rinne et al. 2007, Forbrich et al. 2011, Herbst et al. 2011) occurred especially at sites without large open water areas (Godwin et al. 2013).

We assume the process of convective mixing of the water column (e.g. Godwin et al. 2013, Poindexter and Variano 2013, Podgrajsek et al. 2014, Sahlée et al. 2014, Koebsch et al. 2015) to be crucial for the diurnal pattern of CH_4 emissions at our study site. This is indicated by the concurrent timing of convective mixing and daily peak CH_4 emissions and a generally high fractional source area coverage

385 of the open water, which shows higher rates of CH_4 release than emergent vegetation. Furthermore,
386 closed chamber measurements likewise show night-time peak emissions on the shallow lake in
387 summer 2013 (Hoffmann et al. 2015). During the day, CH_4 is trapped in the lower (anoxic) layers of the
388 thermally stratified water column. Due to the heat release of the surface water to the atmosphere in
389 the night the surface water cools down, initiating convective mixing of the water column down to the
390 bottom. Diffusion is enhanced due to the buoyancy-induced turbulence, the associated increased gas
391 transfer velocity at the air-water interface (Eugster et al. 2003, MacIntyre et al. 2010, Podgrajsek et al.
392 2014) as well as the transport of CH_4 enriched bottom water to the surface (Godwin et al. 2013,
393 Podgrajsek et al. 2014). In addition, ebullition can be triggered by turbulence due to convective mixing
394 (Podgrajsek et al. 2014, Read et al. 2012). Apart from convective mixing, highest sediment and soil
395 temperature in the night until early morning might play an important role for the peak emissions of
396 CH_4 due to increased microbial activity. Furthermore, diurnal variability in CH_4 oxidation could
397 contribute to the daily pattern of CH_4 release. Oxygen is supplied to the water, sediment and soil during
398 the day in consequence of photosynthesis and increases CH_4 oxidation. However, convective mixing of
399 the water column during the night might supply oxygen to deeper water depths potentially increasing
400 CH_4 oxidation. We assume plant-mediated transport to be characterised by a reverse diurnal cycle with
401 peak emissions during day-time, as the release of methane is dependent on the stomatal conductance
402 of the plants (e.g. Morrisey et al. 1993). This pathway is limited to plants with aerenchymatic tissue
403 like *Typha latifolia*, which dominates the eulittoral zone at our study site. CH_4 is transported from the
404 soil to the atmosphere, bypassing potential oxidation zones above the rhizosphere (chimney effect).
405 Unusually for wetland plants (Torn and Chapin 1993), complete stomatal closure during night was
406 observed for *Typha latifolia* (Chanton et al. 1993). However, this temporal constraint seems to be
407 superimposed by more efficient CH_4 pathways during the night and early morning. Apart from CH_4,
408 thermally induced convection potentially contributes also to the diurnal fluctuation of the CO_2 flux at
409 our study site. According to Eugster et al. (2003) penetrative convection might be the dominant
410 mechanism yielding CO_2 fluxes during periods of low wind speed, especially in case of a stratification
411 of CO_2 concentrations in the water body. Ebullition triggered by convective mixing might be less
412 important for CO_2 than for CH_4, as concentrations of CO_2 are most often low in gas bubbles (e.g. Casper
413 et al. 2000, Poissant et al. 2007, Repo et al. 2007, Sepulveda-Jauregui et al. 2015, Spawn et al. 2015).
414 Further investigations should focus on the controls of the diurnal patterns in CO_2 and CH_4 exchange
415 based on additional measurements, e.g. gas concentrations in the water, methane oxidation or plant-
416 mediated transport.

4.2 Annual CH_4 emissions

The CH_4 emissions of our studied ecosystem were within the range of other temperate fen sites rewetted for several years (up to 63 g CH_4 m^{-2} a^{-1}; e.g. Hendriks et al. 2007, Wilson et al. 2008, Günther et al. 2013, Schrier-Uijl et al. 2014). This rate is remarkably higher than the emission factor of 28.8 g CH_4 m^{-2} a^{-1} that was assigned to rewetted temperate rich organic soils, which is in turn more than twice the rate of the nutrient-poor complement (IPCC 2014). In contrast, newly rewetted fens emit its multiple. In the first year after flooding, Hahn et al. (2015) observed at a fen site in NE Germany an average net release of 260 g CH_4 m^{-2} a^{-1}, which is 186 times higher than before flooding,. Two years later the CH_4 emissions were considerably lower (40 g CH_4 m^{-2} within the growing season; Koebsch et al. 2015). However, natural (e.g. Bubier et al. 1993, Nilsson et al. 2001) and degraded fens (Hatala et al. 2012, Schrier-Uijl et al. 2014, see also IPCC 2014) release most often less CH_4 than the majority of rewetted fens, with some exceptions (e.g. Huttunen et al. 2003).

The two main surface types open water and emergent vegetation differed substantially in their CH_4 exchange rates. Open water contributed overproportionally to the measured ecosystem fluxes and showed remarkably higher CH_4 release rates (52.6 g CH_4 m^{-2} a^{-1}) than the emergent vegetation stands (13.2 g CH_4 m^{-2} a^{-1}). However, closed-chamber measurements at the shallow lake show an even higher long-term average annual CH_4 release rate (206 g CH_4 m^{-2} a^{-1}) since rewetting with large interannual variability and occasionally extreme high release rates (up to 400 g CH_4 m^{-2} $a^{-}1$; Casares et al., in prep.).

We assume the permanent high inundation and high productivity due to eutrophic conditions, feeding the organic mud deposited at the bottom of the open water body (which is typical for shallow lakes in rewetted fens), to be of particular importance for high CH_4 emissions as substrate for decomposition. The mud initially evolved as a mixture of sand and easily decomposable labile plant litter from reed canary grass, which died-off after flooding and produced a large C pool for CH_4 production (Hahn-Schöfl et al 2011). During an incubation experiment with substrate from our study site Hahn-Schöfl et al. (2011) observed that the new sediment layer has very high specific rates of anaerobic CH_4 (and CO_2) production. In addition, Zak et al. (2015) emphasised the impact of litter quality and reported a very high CH_4 production potential for litter of *Ceratophyllum demersum,* which dominates the biomass in the open water at our study site. Due to the eutrophic character of the lake and associated high productivity within the open water body and in the eulittoral zone, high amounts of fresh labile organic matter continuously replenish the mud layer and thus the C pool. Especially in case of strong winds we further assume a lateral input of allochthonous organic matter into the NE “bay” of the shallow lake, which is the area with the peak contribution of our EC derived fluxes, and thus an additional refill of the C pool. The importance of fresh labile organic matter provided by the die-back of the former

vegetation as driving force for high CH_4 emissions was also discussed in Hahn et al. (2015). They measured the highest CH_4 emissions in sedge stands suffering from strongest die-back.

For comparison annual budgets of CH_4 and CO_2 for other nutrient-rich lentic freshwater ecosystems in terms of pristine, anthropogenically influenced and transient ecosystems are listed in Table 4. Studies on nutrient-rich lakes generally revealed lower CH_4 release for open water. In contrast, beaver ponds were partially reported to emit comparable rates of CH_4. Similarly to our study site beaver ponds are at least in the beginning disbalanced ecosystems due to a rapidly increased water level with associated suffering and finally the die-back of former vegetation, which is not adapted to higher water levels. A large C pool for CH_4 production develops. However, even for a beaver pond existing more than 30 years CH_4 emissions still accounted for 40 g CH_4 m^{-2} a^{-1} (Yavitt et al. 1992).

The lower CH_4 emissions of the surface type emergent vegetation might be the result of increased CH_4 oxidation in the soil, as plants with aerenchymatic tissue release oxygen into the rhizosphere, in reverse to the emission of CH_4 into the atmosphere (Bhullar et al. 2013). Minke et al. (2015) highlight the difference in net CH_4 release for typical helophyte stands with moderate emissions for *Typha* dominated sites. Besides the effect of the gas transport within plants, lower water and sediment temperatures due to shading by the emergent vegetation might yield lower CH_4 production than for open water. Furthermore, the soil of emergent vegetation stands is generally only temporarily and partly inundated and the water table decreased additionally during the unusual warm and dry summer 2013, probably resulting in a lower rate of anaerobic decomposition to CH_4 and a higher rate of CH_4 oxidation in the aerated top soil. This in turn might be a reason, that in comparison to other sites dominated by *Typha* (rewetted wetlands, lake shores and freshwater marshes; see Table 4) the emergent vegetation at our site is at the lower limit of reported CH_4 release rates and best comparable to closed chamber measurements of *Typha latifolia* microsites at another rewetted fen site in NE Germany (Günther et al. 2015).

4.3 Annual net CO_2 release

We observed high annual net release of CO_2 during the observation period, which is rather uncommon for fens several years after rewetting (e.g. Hendriks et al. 2007, Schrier-Uijl et al. 2014, Knox et al. 2015). Surprisingly, the net CO_2 budget was higher or similar to those of some drained and degraded peatlands (e.g. Hatala et al. 2012, Schrier-Uijl et al. 2014, but IPCC 2014). Both surface types acted as net sources, with emergent vegetation (750 g CO_2 m^{-2} $a^{-}1$) showing a distinctively higher net budget (158 g CO_2 m^{-2} a^{-1}) as well as GPP and R_{eco} rates than open water. Only few NEE rates are published for the open water body of eutrophic shallow lakes. Ducharme-Riel et al. (2015) report 224 g CO_2 m^{-2} a^{-1} as annual NEE of a eutrophic lake in Canada (see Table 4). According to Kortelainen et al. (2006) Finnish

lakes, which are mainly small and shallow, continuously emit CO_2 during the ice-free period, positively correlated with their trophic state.

Our study revealed a high annual net CO_2 release for emergent vegetation, which is in the wide range of NEE rates for *Typha* sites reported in other studies, including both net CO_2 sources and sinks (see Table 5). GPP and R_{eco} are generally high (especially at rewetted fen sites; both component fluxes most often > 3000 g CO_2 m^{-2} a^{-1}), characterising *Typha* stands as high turnover sites, usually resulting in net CO_2 uptake. In contrast, R_{eco} and GPP rates at our study site are in the lower part of the reported range. We assume the continuously high R_{eco} rates during winter 2013/2014, contributing to the high annual net CO_2 emissions, to be the result of mild and dry meteorological conditions. In summer 2013, R_{eco} exceeded GPP already in late June, indicating a significant contribution of heterotrophic respiration to the CO_2 production. Unusual warm and dry conditions and associated water table lowering during summer 2013 might have triggered a shift from anaerobic to aerobic decomposition due to the exposure of formerly only shallowly inundated soil and organic mud, primarily in the emergent vegetation stands. We could not observe a considerable decrease of the spatial extent of the open water body as emergent vegetation mainly covers the shallower edges of the water body. The effect of water table lowering at *Typha* sites due to dry conditions is also shown by Günther et al. (2015) and Chu et al. (2015): relative increase of R_{eco} rates, resulting in net CO_2 release. This might be of special interest in terms of climate change, as a temperature increase and significantly less precipitation in summer are expected for NE Germany and meteorological conditions are more frequently characterised as “unusually” warm and dry. In addition, a considerable increase of microbial activity and thus, generally increased decomposition due to high temperatures might be of importance. Besides CH_4, Hahn-Schöfl et al. (2011) showed that the new sediment layer at the bottom of inundated areas exhibits very high rates of anaerobic CO_2 production. Allochthonous organic matter import into the NE bay due to lateral transport, as discussed for CH_4, might have further enhanced decomposition (e.g. Chu et al. 2015). Longer data gaps in summer 2013 (see Fig. A1) increase the uncertainty of our annual CO_2 budget. However, the observed shift to net CO_2 release starting in late June 2013 as well as its continuation later on are substantially based on measurements.

4.4 Global warming potential and the impact of spatial heterogeneity

The lake ecosystem is characterised by a strong climate impact 9 years after rewetting, mainly driven by high CH_4 emissions. Based on our results the site can hardly be classified into any rewetting phase of the concept discussed by Augustin and Joosten (2007). Our results imply a delayed shift of the ecosystem towards a C sink with reduced climate impact, which might be the result of the exceptional characteristics represented by eutrophic conditions and lateral transport of organic matter within the open water body. The trophic status of water and sediment is an important factor regulating GHG

emissions, as shown by Schrier-Uijl et al. (2011) for lakes and drainage ditches in wetlands. However, the unusual meteorological conditions during our study period might have caused a differing (lower or higher) GWP compared to previous years. CH_4 emissions might have been lower at the expense of high net CO_2 release, whereas under usual meteorological conditions e.g. CO_2 uptake could probably compensate the CH_4 emissions. Inundation is generally associated with high CH_4 emission. Thus, during rewetting the water table is generally recommended to be held at or just below the soil surface to prevent inundation and the formation of organic mud (Couwenberg et al. 2011, Joosten et al. 2012, Zak et al. 2015).

In contrast to CH_4, the influence of water level on net CO_2 release is not nearly consistent in the few existing studies of rewetted peatlands. In comparison to our site Knox et al. (2015) reported high net CO_2 uptake to substantially compensate high CH_4 emissions for a site with mean water levels above the soil surface after several years of rewetting (see Table 5). Similarly, Schrier-Uijl et al. (2014) reported high CO_2 uptake rates for a Dutch fen site 7 years after rewetting and even C uptake and a GHG sink function after 10 years with water levels below or at the soil surface. Herbst et al. (2011) present a snapshot of the GHG emissions of a Danish site after 5 years of rewetting with permanently and seasonally wet areas, whereby high CO_2 uptake and moderate CH_4 emissions lead to substantial GHG savings. In contrast, weak CO_2 uptake and decreasing, but still high CH_4 emissions were reported for another fen site in NE Germany with mean water levels above the soil surface (Koebsch et al. 2013, 2015 and Hahn et al. 2015), resulting in a decreasing climate impact after 3 years of rewetting. Interestingly, changes of NEE due to flooding were negligible, although GPP and R_{eco} rates decreased considerable due to the flooding (Koebsch et al. 2013). In comparison to the decreasing CH_4 emissions at this site, Waddington and Day (2007) report enhancing CH_4 release for a Canadian peatland in the first 3 years after rewetting. A third rewetted fen site in NE Germany with water levels close to the soil surface was reported as weak GHG source 14-15 years after rewetting (Günther et al. 2015).

We calculated the “true” fluxes of CO_2 and CH_4 for the AOI by weighting the NLR functions for the two surface types with their fractional coverage inside the AOI. The inferred C budget and global warming potential differs considerably from that of the EC source area, highlighting the strikingly different emission rates of open water versus emergent vegetation. Thus, footprint analysis providing the fractional coverage of the main surface types is imperative for the interpretation of ecosystem flux measurements as provided by the EC technique at such a spatially heterogeneous site. In addition, for an interannual comparison of EC derived budgets for such sites it is necessary to define a fixed AOI, as the cumulative footprint climatology (representing the EC source area) changes interannualy. Inter-site comparisons (e.g. with other shallow lakes evolved during fen rewetting) are challenging with regard to the site-specific spatial heterogeneity and their interannual variability, if short-term studies

like the present one are involved. Comparisons might be misleading in case the fractional coverages of the main surface types are not considered. Furthermore, as shown by Wilson et al. (2007, 2008) and Minke et al. (2015) vegetation composition has a remarkable effect on GHG emissions of rewetted peatlands and should be considered within inter-site comparisons.

5 Conclusions

This study contributes to the understanding of eutrophic shallow lakes as a challenging ecosystem often evolving during fen rewetting. Within the study period the ecosystem was a strong source of CH_4 and CO_2. Both open water and emergent vegetation, particularly including the eulittoral zone, were net emitters of CH_4 and CO_2, but with strikingly different release rates. This illustrates the importance of footprint analysis for the interpretation of the EC measurements on a rewetted site with distinct spatial heterogeneity. The strong climate impact of the lake is dominated by considerable CH_4 release, particularly from the open water section. A comparison with existing chamber measurements at the open water body for the same time period will be helpful for the evaluation of our measurements and estimation of the surface type fluxes. The site is gradually changing, with helophytes (especially *Typha latifolia*) progressively entering the open water body in the course of terrestrialisation. Peat formation and C uptake might be initiated once the shallow lake is inhabited by peat-forming vegetation and replenished by organic sediments. Therefore, long-term measurements are necessary to evaluate the impact of future ecosystem development on GHG emissions. Interannual comparisons are also necessary to verify what the results of this study imply: that the intended effects of rewetting in terms of CO_2 emission reduction and C sink recovery are not yet achieved at this site. In this context, the effect of unusual meteorological conditions needs further investigation. More general statements for the climate impact of rewetted fens can only be provided by inclusion of additional sites varying e.g. in groundwater table and plant composition. We assume that shallow lakes represent a special case with regard to the GHG dynamics and climate impact, with exceptionally high CH_4 release and occasionally high net CO_2 emissions. Our study shows that permanent (high) inundation in combination with nutrient-rich conditions involves the risk of long-term high CH_4 emissions. They counteract the actually intended lowering of the climate impact of drained and degraded fens and can result in an even stronger climate impact than degraded fens, as also shown in previous studies. We strongly recommend to consider this risk in future rewetting projects and support the call of Lamers et al. (2015) for the need of well-conceived restoration management instead of the trial-and-error approach, whereon restoration of wetland ecosystem services was based for a long time.

Appendix A

Measurement data coverage of CO_2 and CH_4 fluxes within the study period is shown in Fig. A1.

Data availability

Processed eddy covariance flux and meteorological data of this study site (site code DE-Zrk) are available at http://www.europe-fluxdata.eu.

Acknowledgements

This work was supported by the Helmholtz Association of German Research Centres through a Helmholtz Young Investigators Group to T.S. (grant VH-NG-821) and is a contribution to the Helmholtz Climate Initiative REKLIM (Regional Climate Change). Infrastructure funding through the Terrestrial Environmental Observatories Network (TERENO) is also acknowledged. We thank M. Hoffmann (ZALF, Müncheberg, Germany) and C. Hohmann (GFZ Potsdam, Germany) for providing meteorological data.

References

Aubinet, M., Feigenwinter, C., Heinesch, B., Laffineur, Q., Papale, D., Reichstein, M., Rinne, J. and Van Gorsel, E.: Nighttime flux correction, in: Eddy Covariance: A practical guide to measurement and data analysis, Springer Atmospheric Sciences, edited by Aubinet, M., Vesala, T. and Papale, D., Springer Netherlands, Dordrecht, doi:10.1007/978-94-007-2351-1, 133-158, 2012.

Augustin, J. and Joosten, H.: Peatland rewetting and the greenhouse effect, International Mire Conservation Group Newsletter, 3, 29-30, 2007.

Barcza, Z., Kern, A., Haszpra, L. and Kljun, N.: Spatial representativeness of tall tower eddy covariance measurements using remote sensing and footprint analysis, Agr. Forest Meteorol., 149, 795-807, doi: 10.1016/j.agrformet.2008.10.021, 2009.

Bastviken, D., Cole, J., Pace, M. and Tranvik, L.: Methane emissions from lakes: Dependence of lake characteristics, two regional assessments, and a global estimate, Global Biogeochem. Cy., 18, GB4009, doi: 10.1029/2004GB002238, 2004.

Beetz, S., Liebersbach, H., Glatzel, S., Jurasinski, G., Buczko, U. and Höper, H.: Effects of land use intensity on the full greenhouse gas balance in an Atlantic peat bog, Biogeosciences, 10, 1067-1082, doi:10.5194/bg-10-1067-2013, 2013.

Berg, E., Jeschke, L. and Lenschow, U.: Das Moorschutzkonzept Mecklenburg-Vorpommern, Telma, 30, 173-220, 2000.

Béziat, P., Ceschia, E. and Dedieu, G.: Carbon balance of a three crop succession over two cropland sites in South West France, Agr. Forest Meteorol., 149, 1628-1645, doi:10.1016/j.agrformet.2009.05.004, 2009.

Bhullar, G. S., Edwards, P. J. and Olde Venterink, H.: Variation in the plant-mediated methane transport and its importance for methane emission from intact wetland peat mesocosms, J. Plant Ecol., 6, 298-304, doi: 10.1093/jpe/rts045, 2013.

Bignell, N.: The effect of dissolved air on the density of water, Metrologia, 19, 57-59, 1983.

Bonneville, M.-C., Strachan, I. B., Humphreys, E. R. and Roulet, N. T.: Net ecosystem CO_2 exchange in a temperate cattail marsh in relation to biophysical properties, Agr. Forest Meteorol., 148, 69-81, doi:10.1016/j.agrformet.2007.09.004, 2008.

Bubier, J. L., Moore, T. R. and Roulet, N. T.: Methane emissions from wetlands in the Midboreal Region of Northern Ontario, Canada, Ecology, 74, 2240-2254, 1993.

628 Casper, P., Maberly, S. C., Hall, G. H. and Finlay, B. J.: Fluxes of methane and carbon dioxide from a
629 small productive lake to the atmosphere, Biogeochemistry, 49, 1-19, doi:
630 10.1023/A:1006269900174, 2000.

631 Chanton, J. P., Whiting, G. J., Happell, J. D. and Gerard, G.: Contrasting rates and diurnal patterns of
632 methane emission from different types of vegetation, Aquat. Bot., 46, 111-128, 1993.

633 Chen, B., Coops, N. C., Fu, D., Margolis, H. A., Amiro, B. D., Barr, A. G., Black, T. A., Arain, M. A., Bourque,
634 C. P.-A., Flanagan, L. B., Lafleur, P. M., McCaughey, J. H. and Wofsy, S. C.: Assessing eddy-
635 covariance flux tower location bias across the Fluxnet-Canada Research Network based on remote
636 sensing and footprint modelling, Agr. Forest Meteorol., 151, 87–100,
637 doi:10.1016/j.agrformet.2010.09.005, 2011.

638 Chu, H., Gottgens, J. F., Chen, J., Sun, G., Desai, A. R., Ouyang, Z., Shao, C. and Czajkowski, K.: Climatic
639 variability, hydrologic anomaly, and methane emission can turn productive freshwater marshes
640 into net carbon sources, Glob. Change Biol., 21, 1165-1181, doi: 10.1111/gcb.12760, 2015.

641 Couwenberg, J., Thiele, A., Tanneberger, F., Augustin, J., Bärisch, S., Dubovik, D., Liashchynskaya, N.,
642 Michaelis, D., Minke, M., Skuratovich, A. and Joosten, H.: Assessing greenhouse gas emissions
643 from peatlands using vegetation as a proxy, Hydrobiologia, 674, 67-89, doi:10.1007/s10750-011-
644 0729-x, 2011.

645 Dengel, S., Levy, P. E., Grace, J., Jones, S. K. and Skiba, U. M.: Methane emissions from sheep pasture,
646 measured with an open-path eddy covariance system, Glob. Change Biol., 17, 3524-3533, doi:
647 10.1111/j.1365-2486.2011.02466.x, 2011.

648 Ducharme-Riel, V., Vachon, D., del Giorgio, P. A. and Prairie, Y. T.: The relative contribution of winter
649 under-ice and summer hypolimnetic CO_2 accumulation to the annual CO_2 emissions fromn
650 northern lakes, Ecosystems, 18, 547-559, doi:10.1007/s10021-015-9846-0, 2015.

651 Eugster, W., Kling, G., Jonas, T., McFadden, J. P., Wüest, A., MacIntyre, S. and Chapin III, F. S.: CO_2
652 exchange between air and water in an Arctic Alaskan and midlatitude Swiss lake: importance of
653 convective mixing, J. Geophys. Res., 108, 4362, doi: 10.1029/2002JD002653, 2003.

654 Falge, E., Baldocchi, D., Olson, R. J., Anthoni, P., Aubinet, M., Bernhofer, C., Burba, G., Ceulemans, R.,
655 Clement, R., Dolman, H., Granier, A., Gross, P., Grünwald, T., Hollinger, D., Jensen, N.-O., Katul, G.,
656 Keronen, P., Kowalski, A., Ta Lai, C., Law, B. E., Meyers, T., Moncrieff, J., Moors, E., Munger, J. W.,
657 Pilegaard, K., Rannik, Ü., Rebmann, C., Suyker, A., Tenhunen, J., Tu, K., Verma, S., Vesala, T.,
658 Wilson, K. and Wofsy, S. C.: Gap filling strategies for defensible annual sums of net ecosystem
659 exchange, Agr. Forest Meteorol., 107, 43–69, doi:10.1016/S0168-1923(00)00225-2, 2001.

660 Fan, S.-M., Wofsy, S. C., Bakwin, P. S., Jacob, D. J. and Fitzjarrald, D. R.: Atmosphere-biosphere
661 exchange of CO_2 and O_3 in the Central Amazon Forest, J. Geophys. Res., 95, 16851-16864, 1990.

662 Finkelstein, P. L. and Sims, P. F.: Sampling error in eddy correlation flux measurements, J. Geophys.
663 Res.-Atmos., 106, 3503-3509, doi:10.1029/2000JD900731, 2001.

664 Finnigan, J. J., Clement, R., Mahli, Y., Leuning, R. and Cleugh, H. A.: A re-evaluation of long-term flux
665 measurement techniques. Part I: Averaging and coordinate rotation, Bound.-Lay. Meteorol., 107,
666 1-48, doi:10.1023/A:1021554900225, 2003.

667 Forbrich, I., Kutzbach, L., Wille, C., Becker, T., Wu, J. and Wilmking, M.: Cross-evaluation of
668 measurements of peatland methane emissions on microform and ecosystem scales using high-
669 resolution landcover classification and source weight modelling, Agr. Forest Meteorol., 151, 864-
670 874, doi:10.1016/j.agrformet.2011.02.006, 2011.

671 Fratini, F., Ibrom, A., Arriga, N., Burba, G. and Papale, D.: Relative humidity effects of water vapour
672 fluxes measured with closed-path eddy-covariance systems with short sampling lines, Agr. Forest
673 Meteorol., 165, 53-63, 2012.

674 Frolking, S., Talbot, J., Jones, M. C., Treat, C. C., Kauffman, J. B., Tuittila, E.-S. and Roulet, N. T.: Peatlands
675 in the earth´s 21st century climate system, Environ. Rev., 19, 371-396, doi:10.1139/a11-014, 2011.

676 Göckede, M., Rebmann, C. and Foken, T.: A combination of quality assessment tools for eddy
677 covariance measurements with footprint modelling for the characterisation of complex sites, Agr.
678 Forest Meteorol., 127, 175-188, doi:10.1016/j.agrformet.2004.07.012, 2004.

679 Godwin, C. M., McNamara, P. J. and Markfort, C. D.: Evening methane emission pulses from a boreal
680 wetland correspond to convective mixing in hollows, J. Geophys. Res.-Biogeo., 118, 994-1005, doi:
681 10.1002/jgrg.20082, 2013.

682 Günther, A. B., Huth, V., Jurasinski, G. and Glatzel, S.: Scale-dependent temporal variation in
683 determining the methane balance of a temperate fen, Greenhouse Gas Measurement and
684 Management, 4, 41-48, doi: 10.1080/20430779.2013.850395, 2013.

685 Günther, A. B., Huth, V., Jurasinski, G. and Glatzel, S.: The effect of biomass harvesting on greenhouse
686 gas emissions from a rewetted temperate fen, GCB Bioenergy, 7, 1092-1106, doi:
687 10.1111/gcbb.12214, 2015.

688 Hahn, J., Köhler, S., Glatzel, S. and Jurasinski, G.: Methane exchange in a coastal fen in the first year
689 after flooding – A systems shift, PLoS ONE, 10, e0140657, doi:10.1371/journal.pone.0140657,
690 2015.

691 Hahn-Schöfl, M., Zak, D., Minke, M., Gelbrecht, J., Augustin, J. and Freibauer, A.: Organic sediment
692 formed during inundation of a degraded fen grassland emits large fluxes of CH_4 and CO_2,
693 Biogeosciences, 8, 1539-1550, doi:10.5194/bg-8-1539-2011, 2011.

694 Hatala, J., Detto, M., Sonnentag, O., Deverel, S. J., Verfaillie, J. and Baldocchi, D. D.: Greenhouse gas
695 (CO_2, CH_4, H_2O) fluxes from drained and flooded agricultural peatlands in the Sacramento-San
696 Joaquin Delta, Agr. Ecosyst. Environ., 150, 1-18, doi:10.1016/j.agee.2012.01.009, 2012.

697 Hatala Matthes, J., Sturtevant, C., Verfaillie, J., Knox, S. and Baldocchi, D.: Parsing the variability in CH_4
698 flux at a spatially heterogeneous wetland: Integrating multiple eddy covariance towers with high-
699 resolution flux footprint analysis, J. Geophys. Res.-Biogeo., 119, 1322-1339,
700 doi:10.1002/2014JG002642 2014.

701 Hendriks, D. M. D., van Huissteden, J., Dolman, A. J. and van der Molen, M. K.: The full greenhouse gas
702 balance of an abandoned peat meadow, Biogeosciences, 4, 411-424, doi:10.5194/bg-4-411-2007,
703 2007.

704 Hendriks, D. M. D., van Huissteden, J. and Dolman, A. J.: Multi-technique assessment of spatial and
705 temporal variability of methane fluxes in a peat meadow, Agr. Forest Meteorol., 150, 757-774,
706 doi:10.1016/j.agrformet.2009.06.017, 2010.

707 Herbst, M., Friborg, T., Ringgaard, R. and Soegaard, H.: Interpreting the variations in atmospheric
708 methane fluxes observed above a restored wetland, Agr. Forest Meteorol., 151, 841-853,
709 doi:10.1016/j.agrformet.2011.02.002, 2011.

710 Hoffmann, M., Schulz-Hanke, M., Garcia Alba, J., Jurisch, N., Hagemann, U., Sachs, T., Sommer, M. and
711 Augustin, J.: Technical Note: A simple calculation algorithm to separate high-resolution CH_4 flux
712 measurements into ebullition and diffusion-derived components, Biogeosciences Discussions, 12,
713 12923-12945, doi:10.5194/bgd-12-12923-2015, 2015.

714 Holden, J., Chapman, P. J. and Labadz, J. C.: Artificial drainage of peatlands: hydrological and
715 hydrochemical process and wetland restoration, Prog. Phys. Geog., 28, 95-123,
716 doi:10.1191/0309133304pp403ra, 2004.

717 Hommeltenberg, J., Mauder, M., Drösler, M., Heidbach, K., Werle, P. and Schmid, H. P.: Ecosystem
718 scale methane fluxes in a natural temperate bog-pineforest in southern Germany, Agr. Forest
719 Meteorol., 198-199, 273-284, doi:10.1016/j.agrformet.2014.08.017, 2014.

720 Höper, H., Augustin, J., Cagampan, J. P., Drösler, M., Lundin, L., Moors, E., Vasander, H., Waddington,
721 J. M., and Wilson, D.: Restoration of peatlands and greenhouse gas balances, in: Peatlands and
722 climate change, edited by Strack, M., International Peat Society, Jyväskylä, 182-210, 2008.

Horst, T. W. and Lenschow, D. H.: Attenuation of scalar fluxes measured with spatially-displaced sensors, Bound.-Lay. Meteorol., 130, 275-300, doi:10.1007/s10546-008-9348-0, 2009.

Huttunen, J. T., Nykänen, H., Turunen, J. and Martikainen, P. J.: Methane emissions from natural peatlands in the northern boreal zone in Finland, Fennoscandia, Atmos. Environ., 37, 147-151, doi:10.1016/S1352-2310(02)00771-9, 2003.

IPCC: Climate Change 2013: The physical science basis. Contribution of Working Group I to the Fifth Assessment Report of the Intergovernmental Panel on Climate Change, edited by Stocker, T. F., Qin, D., Plattner, G.-K., Tignor, M. M. B., Allen, S. K., Boschung, J., Nauels, A., Xia, Y., Bex, V. and Midgley, P. M., Cambridge University Press, Cambridge, New York, 1535 pp, doi:10.1017/CBO9781107415324, 2013.

IPCC: 2013 Supplement to the 2006 IPCC Guidelines for National Greenhouse Gas Inventories: Wetlands, edited by Hiraishi, T., Krug, T., Tanabe, K., Srivastava, N., Baasansuren, J., Fukuda, M. and Troxler, T.G., IPCC, Switzerland, 354 pp, 2014.

Itzerott, S.: TERENO (Northeast), Climate station Karlshof, Germany. Deutsches GeoForschungsZentrum GFZ. http://dx.doi.org/10.5880/TERENO.265, 2015.

Joosten, H.: The global peatland CO_2 picture – Peatland status and drainage related emissions in all countries of the world, Wetlands International, Ede, 36 pp, 2010.

Joosten, H., Tapio-Biström, M.-L. and Tol, S. (Eds.): Peatlands – guidance for climate change mitigation through conservation, rehabilitation and sustainable use, 2nd edition, Food and Agriculture Organization of the United Nations and Wetlands International, 100 pp, 2012.

Juutinen, S., Alm, J., Larmola, T., Huttunen, J. T., Morero, M., Martikainen, P. J. and Silvola, J.: Major implication of the littoral zone for methane release from boreal lakes, Global Biogeochem. Cy., 17, 1117, doi:10.1029/2003GB002105, 2003.

Kankaala, P., Ojala, A. and Käki, T.: Temporal and spatial variation in methane emissions from a flodded transgression shore of a boreal lake, Biogeochemistry, 68, 297-311, doi: 10.1023/B:BIOG.0000031030.77498.1f, 2004.

Knox, S. H., Sturtevant, C., Hatala Matthes, J., Koteen, L., Verfaillie, J. and Baldocchi, D.: Agricultural peatland restoration: effects of land-use change on greenhouse gas (CO_2 and CH_4) fluxes in the Sacramento-San Joaquin Delta, Glob. Change Biol., 21, 750-765, doi:10.1111/gcb.12745, 2015.

Koebsch, F., Glatzel, S., Hofmann, J., Forbrich, I. and Jurasinski, G.: CO_2 exchange of a temperate fen during the conversion from moderately rewetting to flooding, J. Geophys. Res.-Biogeo., 118, 940-950, doi:10.1002/jgrg.20069, 2013.

Koebsch, F., Jurasinski, G., Koch, M., Hofmann, J. and Glatzel, S.: Controls for multi-scale temporal variation in ecosystem methane exchange during the growing season of a permanently inundated fen, Agr. Forest Meteorol., 204, 94-105, doi:10.1016/j.agrformet.2015.02.002, 2015.

Kormann, R. and Meixner, F. X.: An analytical footprint model for non-neutral stratification, Bound.-Lay. Meteorol., 99, 207-224, doi:10.1023/A:1018991015119, 2001.

Kortelainen, P., Rantakari, M., Huttunen, J. T., Mattsson, T., Alm, J., Juutinen, S., Larmola, T., Silvola, J. and Martikainen, P. J.: Sediment respiration and lake trophic state are important predictors of large CO_2 evasion from small boreal lakes, Glob. Change Biol., 12, 1554-1567, doi: 10.1111/j.1365-2486.2006.01167.x. 2006.

Lamers, L. P. M., Vile, M. A., Grootjans, A. P., Acreman, M. C., van Diggelen, R., Evans, M. G., Richardson, C. J., Rochefort, L., Koojiman, A. M., Roelofs, J. G. M. and Smolders, A. J. P.: Ecological restoration of rich fens in Europe and North America: from trial and error to an evidence-based approach, Biol. Rev., 90, 182-203, doi: 10.1111/brv.12102, 2015.

Lloyd, J. and Taylor, J. A.: On the temperature dependence of soil respiration, Funct. Ecol., 8, 315-323, doi:10.2307/2389824, 1994.

Lund, M., Lafleur, P. M., Roulet, N. T., Lindroth, A., Christensen, T. R., Aurela, M., Chojnicki, B. H., Flanagan, L. B., Humphreys, E. R., Laurila, T., Oechel, W., Olejnik, J., Rinne, J., Schubert, P. and Nilsson, M. B.: Variability in exchange of CO_2 across 12 northern peatland and tundra sites, Glob. Change Biol., 16, 2436-2448, doi:10.1111/j.1365-2486.2009.02104.x, 2010.

MacIntyre, S., Jonsson, A., Jansson, M., Aberg, J., Turney, D. E. and Miller, S. D.: Buoyancy flux, turbulence, and the gas transfer coefficient in a stratified lake, Geophys. Res. Lett., 37, L24604, doi:10.1029/2010GL044164, 2010.

Mauder, M. and Foken, T.: Documentation and instruction manual of the Eddy covariance software package TK2. Arbeitsergebnisse Nr. 26, University of Bayreuth, Department of Micrometeorology, 42 pp, 2004.

McDermitt, D., Burba, G., Xu, L., Anderson, T., Komissarov, A., Riensche, B., Schedlbauer, J., Starr, G., Zona, D., Oechel, W., Oberbauer, S. and Hastings, S.: A new low-power, open-path instrument for measuring methane flux by eddy covariance, Appl. Phys. B, 102, 391-405, doi:10.1007/s00340-010-4307-0, 2011.

Meyer, K., Höper, H. and Blankenburg, J.: Spurengashaushalt und Klimabilanz von Niedermooren unter dem Einfluß des Vernässungsmanagements, in: Ökosystemmanagement für Niedermoore.

Strategien und Verfahren zur Renaturierung, edited by Kratz, R. and Pfadenhauer, J., Ulmer, Stuttgart, 104-111, 2001.

Minke, M., Augustin, J., Burlo, A., Yarmashuk, T., Chuvashova, H., Thiele, A., Freibauer, A., Tikhonov, V. and Hoffmann, M.: Water level, vegetation composition and plant productivity explain greenhouse gas fluxes in temperate cutover fens after inundation, Biogeosciences Discussions, 12, 17393-17452, doi:10.5194/bgd-12-17393-2015, 2015.

Moffat, A. M., Papale, D., Reichstein, M., Hollinger, D. Y., Richardson, A. D., Barr, A. G., Beckstein, C., Braswell, B. H., Churkina, G., Desai, A. R., Falge, E., Gove, J. H., Heimann, M., Hui, D., Jarvis, A. J., Kattge, J., Noormets, A. and Stauch, V. J.: Comprehensive comparison of gap-filling techniques for eddy covariance net carbon fluxes, Agr. Forest Meteorol., 147, 209-232, doi:10.1016/j.agrformet.2007.08.011, 2007.

Moncrieff, J. B., Clement, R., Finnigan, J. and Meyers, T.: Averaging, detrending and filtering of eddy covariance time series, in: Handbook of micrometeorology: a guide for surface flux measurements, edited by Lee, X., Massman, W. J. and Law, B. E., Kluwer Academic, Dordrecht, 7-31, doi:10.1007/1-4020-2265-4, 2004.

Morrisey, L. A., Zobel, D. B. and Livingston, G. P.: Significance of stomatal control on methane release from Carex-dominated wetlands, Chemosphere, 26, 339-355, doi:10.1016/0045-6535(93)90430-D, 1993.

Naiman, R. J., Manning, T. and Johnston, C. A.: Beaver population fluctuations and tropospheric methane emissions in boreal wetlands, Biogeochemistry, 12, 1-15, doi: 10.1007/BF00002623, 1991.

Nilsson, M., Mikkelä, C., Sundh, I., Granberg, G., Svensson, B. H. and Ranneby, B.: Methane emission from Swedish mires: National and regional budgets and dependence on mire vegetation, J. Geophys. Res., 106, 20847-20860, doi:10.1029/2001JD900119, 2001.

Petrescu, A. M. R., Lohila, A., Tuovinen, J.-P., Baldocchi, D. D., Desai, A. R., Roulet, N. T., Vesala, T., Dolman, A. J., Oechel, W. C., Marcolla, B., Friborg, T., Rinne, J., Hatala Matthes, J., Merbold, L., Meijide, A., Kiely, G., Sottocornola, M., Sachs, T., Zona, D., Varlagin, A., Lai, D. Y. F., Veenendaal, E., Parmentier, F.-J. W., Skiba, U., Lund, M., Hensen, A., van Huissteden, J., Flanagan, L. B., Shurpali, N. J., Grünwald, T., Humphreys, E. R., Jackowicz-Korczyński, M., Aurela, M. A., Laurila, T., Grüning, C., Corradi, C. A. R., Schrier-Uijl, A. P., Christensen, T. R., Tamstorf, M. P., Mastepanov, M., Martikainen, P. J., Verma, S. B., Bernhofer, C. and Cescatti, A.: The uncertain climate footprint of wetlands under human pressure, PNAS, 112, 4594-4599, doi:10.1073/pnas.1416267112, 2015.

818 Podgrajsek, E., Sahlée, E. and Rutgersson, A.: Diurnal cycle of lake methane flux, J. Geophys. Res.-
819 Biogeo., 119, 236-248, doi:10.1002/2013JG002327, 2014.

820 Poindexter, C. M. and Variano, E. A.: Gas exchange in wetlands with emergent vegetation: the effects
821 of wind and thermal convection at the air–water interface, J. Geophys. Res.-Biogeo., 118, 1297–
822 1306, doi:10.1002/jgrg.20099, 2013.

823 Poissant, L., Constant, P., Pilote, M., Canário, J., O'Driscoll, N., Ridal, J. and Lean, D.: The ebullition of
824 hydrogen, carbon monoxide, methane, carbon dioxide and total gaseous mercury from the
825 Cornwall Area of Concern, Sci. Total Envir., 381, 256-262, doi:10.1016/j.scitotenv.2007.03.029,
826 2007.

827 R Core Team: R: A Language and Environment for Statistical Computing. R Foundation for Statistical
828 Computing, Vienna, Austria, 2012.

829 Read, J. S., Hamilton, D. P., Desai, A. R., Rose, K. C., MacIntyre, S., Lenters, J. D., Smyth, R. L., Hanson,
830 P. C., Cole, J. J., Staehr, P. A., Rusak, J. A., Pierson, D. C., Brookes, J. D., Laas, A. and Wu, C. H.: Lake-
831 size dependency of wind shear and convection as controls on gas exchange, Geophys. Res. Lett.,
832 39, L09405, doi:10.1029/2012GL051886, 2012.

833 Reichstein, M., Falge, E., Baldocchi, D., Papale, D., Aubinet, M., Berbigier, P., Bernhofer, C., Buchmann,
834 N., Gilmanov, T., Granier, A., Grünwald, T., Havránková, K., Ilvesniemi, H., Janous, D., Knohl, A.,
835 Laurila, T., Lohila, A., Loustau, D., Matteucci, G., Meyers, T., Miglietta, F., Ourcival, J.-M.,
836 Pumpanen, J., Rambal, S., Rotenberg, E., Sanz, M., Tenhunen, J., Seufert, G., Vaccari, F., Vesala, T.,
837 Yakir, D. and Valentini, R.: On the separation of net ecosystem exchange into assimilation and
838 ecosystem respiration: review and improved algorithm, Glob. Change Biol., 11, 1424-1439,
839 doi:10.1111/j.1365-2486.2005.001002.x, 2005.

840 Repo, M. E., Huttunen, J. T., Naumov, A. V., Chichulin, A. V., Lapshina, E. D., Bleuten, W. and
841 Martikainen, P. J.: Release of CO_2 and CH_4 from small wetland lakes in western Siberia, Tellus, 59B,
842 788-796, doi:10.1111/j.1600-0889.2007.00301.x, 2007.

843 Rinne, J., Riutta, T., Pihlatie, M., Aurela, M., Haapanala, S., Tuovinen, J.-P., Tuittila, E.-S. and Vesala, T.:
844 Annual cycle of methane emission from a boreal fen measured by the eddy covariance technique,
845 Tellus, 59B, 449-457, doi:10.1111/j.1600-0889.2007.00261.x, 2007.

846 Rocha, A. V. and Goulden, M. L.: Large interannual CO_2 and energy exchange variability in a freshwater
847 marsh under consistent environmental conditions, J. Geophys. Res., 113, G04019,
848 doi:10.1029/2008JG000712, 2008.

Rõõm, E.-I., Nõges, P., Feldmann, T., Tuvikene, L., Kisand, A., Teearu, H. and Nõges, T.: Years are not brothers: Two-year comparison of greenhouse gas fluxes in large shallow Lake Võrtsjärv, Estonia, J. Hydrol., 519, 1594-1606, doi:10.1016/j.jhydrol.2014.09.011, 2014.

Roulet, N. T., Ash, R. and Moore, T. R.: Low boreal wetlands as a source of atmospheric methane, J. Geophys. Res., 97, 3739-3749, 1992.

Roulet, N.T., Ash, R., Quinton, W. and Moore, T. R.: Methane flux from drained northern peatlands: Effect of a persistent water tale lowering on flux, Global Biogeochem. Cy., 7, 749-769, doi:10.1029/93GB01931, 1993.

Sahlée, E., Rutgersson, A., Podgrajsek, E. and Bergström, H.: Influence from surrounding land on the turbulence measurements above a lake, Bound.-Lay. Meteorol., 150, 235-258, doi:10.1007/s10546-013-9868-0, 2014.

Schrier-Uijl, A. P., Veraart, A. J., Leffelaar, P. A., Berendse, F. and Veenendaal, E. M.: Release of CO_2 and CH_4 from lakes and drainage ditches in temperate wetlands, Biogeochemistry, 102, 265-279, doi:10.1007/s10533-010-9440-7, 2011.

Schrier-Uijl, A. P., Kroon, P. S., Hendriks, D. M. D., Hensen, A., van Huissteden, J., Berendse, F. and Veenendaal, E. M.: Agricultural peatlands: towards a greenhouse gas sink – a synthesis of a Dutch landscape study, Biogeosciences, 11, 4559-4576, doi:10.5194/bg-11-4559-2014, 2014.

Sepulveda-Jauregui, A., Walter Anthony, K. M., Martinez-Cruz, K., Greene, S. and Thalasso, F.: Methane and carbon dioxide emissions from 40 lakes along a north-south latitudinal transect in Alaska, Biogeosciences, 12, 3197-3223, doi:10.5194/bg-12-3197-2015, 2015.

Shoemaker, W. B., Anderson, F., Barr, J. G., Graham, S. L. and Botkin, D. B.: Carbon exchange between the atmosphere and subtropical forested cypress and pine wetlands, Biogeosciences, 12, 2285-2300, doi:10.5194/bg-12-2285-2015, 2015.

Siebicke, L., Hunner, M. and Foken, T.: Aspects of CO_2 advection measurements, Theor. Appl. Climatol., 109, 109-131, doi:0.1007/s00704-011-0552-3, 2012.

Silvius, M., Joosten, H. and Opdam, S.: Peatlands and people, in: Assessment on peatlands, biodiversity and climate change: Main Report, edited by Parish, F., Sirin, A., Charman, D., Joosten, H., Minayeva, T., Silvius, M. and Stringer, L., Global Environment Centre, Kuala Lumpur, and Wetlands International, Wageningen, 20-38, 2008.

Smith, L. K. and Lewis Jr., W. M.: Seasonality of methane emissions from five lakes and associated wetlands of the Colorado Rockies, Global Biogeochem. Cy., 6, 323-338, 1992.

880 Spawn, S. A., Dunn, S. T., Fiske, G. J., Natali, S. M., Schade, J. D. and Zimov, N. S.: Summer methane
881 ebullition from a headwater catchment in Northeastern Siberia, Inland Waters, 5, 224-230,
882 doi:10.5268/IW-5.3.845, 2015.

883 Steffenhagen, P., Zak, D., Schulz, K., Timmermann, T. and Zerbe, S.: Biomass and nutrient stock of
884 submersed and floating macrophytes in shallow lakes formed by rewetting of degraded fens,
885 Hydrobiologia, 692, 99-109, doi:10.1007/s10750-011-0833-y, 2012.

886 Strachan, I. B., Nugent, K. A., Crombie, S. and Bonneville, M.-C.: Carbon dioxide and methane exchange
887 at a cool-temperate freshwater marsh, Environ. Res. Lett., 10, 065006, doi:10.1088/1748-
888 9326/10/6/065006, 2015.

889 Succow, M.: Durchströmungsmoore, in: Landschaftsökologische Moorkunde, edited by Succow, M.
890 and Joosten, H., Schweizerbart, Stuttgart, 463-470, 2001.

891 Torn, M. S. and Chapin III, F. S.: Environmental and biotic controls over methane flux from arctic tundra,
892 Chemosphere, 26, 357-368, doi:10.1016/0045-6535(93)90431-4, 1993.

893 van Dijk, A., Moene, A. F. and de Bruin, H. A. R.: The principles of surface flux physics: Theory, practice
894 and description of the ECPack library, Meteorology and Air Quality Group, Wageningen University,
895 Wageningen, 98 pp, 2004.

896 Vickers, D. and Mahrt, L.: Quality control and flux sampling problems for tower and aircraft data, J.
897 Atmos. Ocean. Tech., 14, 512-526, 1997.

898 Waddington, J. M. and Day, S. M.: Methane emissions from a peatland following restoration, J.
899 Geophys. Res., 112, G03018, doi:10.1029/2007JG000400, 2007.

900 Wagner, W. and Pruß, A.: The IAPWS formulation 1995 for the thermodynamic properties of ordinary
901 water substance for general and scientific use, J. Phys. Chem. Ref. Data**,** 31, 387-535, 2002.

902 Wang, H., Lu, J., Wang, W., Yang, L. and Yin, C.: Methane fluxes from the littoral zone of hyper eutrophic
903 Taihu Lake China, J. Geophys. Res., 111, D17109, doi:10.1029/2005JD006864, 2006.

904 Webb, E. K., Pearman, G. I. and Leuning. R.: Correction of flux measurements for density effects due
905 to heat and water vapor transfer, Q. J. Roy. Meteor. Soc., 106, 85-100,
906 doi:10.1002/qj.49710644707, 1980.

907 Whiting, G. J. and Chanton, J. P.: Greenhouse carbon balance of wetlands: methane emission versus
908 carbon sequestration, Tellus, 53B, 521-528, doi: 10.1034/j.1600-0889.2001.530501.x, 2001.

909 Wilczak, J. M., Oncley, S. P. and Stage, S. A.: Sonic anemometer tilt correction algorithms, Bound.-Lay.
910 Meteorol., 99, 127-150, doi:10.1023/A:1018966204465, 2001.

911 Wilson, D., Tuittila, E.-S., Alm, J., Laine, J., Farrell, E. P. and Byrne, K. A.: Carbon dioxide dynamics of a
912 restored maritime peatland, Ecoscience 14, 71-80, doi: 10.2980/1195-
913 6860(2007)14[71:CDDOAR]2.0.CO;2, 2007.

914 Wilson, D., Alm, J., Laine, J., Byrne, K. A., Farrell, E. P. and Tuittila, E.-S.: Rewetting of cutaway
915 peatlands: are we re-creating hot plots of methane emissions?, Restor. Ecol., 17, 796-806,
916 doi:10.1111/j.1526-100X.2008.00416.x, 2008.

917 Yavitt, J. B., Angell, L. L., Fahey, T. J., Cirmo, C. P. and Driscoll, C. T.: Methane fluxes, concentrations,
918 and production in two Adirondack beaver impoundments, Limnol. Oceanogr., 37, 1057-1066,
919 1992.

920 Zak, D., Gelbrecht, J., Wagner, C. and Steinberg, C. E. W.: Evaluation of phosphorus mobilisation
921 potential in rewetted fens by an improved sequential chemical extraction procedure, Eur. J. Soil.
922 Sci., 59, 1191-1201, doi:10.1111/j.1365-2389.2008.01081.x, 2008.

923 Zak, D., Reuter, H., Augustin, J., Shatwell, T., Barth, M., Gelbrecht, J. and McInnes, R. J.: Changes of the
924 CO_2 and CH_4 production potential of rewetted fens in the perspective of temporal vegetation
925 shifts, Biogeosciences, 12, 2455-2468, doi:10.5194/bg-12-2455-2015, 2015.

926 Zerbe, S., Steffenhagen, P., Parakenings, K., Timmermann, T., Frick, A., Gelbrecht, J. and Zak, D.:
927 Ecosystem service restoration after 10 years of rewetting peatlands in NE Germany, Environ.
928 Manage., 51, 1194-1209, doi:10.1007/s00267-013-0048-2, 2013.

929 Zhu, D., Chen, H., Zhu, Q., Wu, Y. and Wu, N.: High Carbon Dioxide Evasion from an Alpine Peatland
930 Lake: The Central Role of Terrestrial Dissolved Organic Carbon Input, Water Air Soil Poll., 223,
931 2563-2569, doi:10.1007/s11270-011-1048-6, 2012.
932

933 Table 1: Data loss and final data coverage during the observation period. CO_2 and CH_4 flux data were
934 lost by power and instrument failure and maintenance as well as quality control and footprint analysis.

Filter criteria	**Percentage of data [%]**	
	CO_2	**CH_4**
Power and instrument failure, maintenance	15.0	46.4
Absence of sensor	-	11.2
QC 2	7.5	2.0
RSSI	-	2.1
u*	18.6	8.8
Unreasonably high fluxes	0.2	0.1
No footprint information/footprint > 20 % outside the AOI	13.2	6.5
Final data coverage	**45.5**	**22.9**

935

Table 2: Gapfilling model performance was estimated according to Moffat et al. (2007) with several measures (n_{CO2} = 6193, n_{CH4} = 3386, fluxes of best quality QC 0): the adjusted coefficient of determination R^2_{adj} for phase correlation (significant in all cases, p-value < $2.2e^{-16}$), the absolute root mean square index ($RMSE_{abs}$) and the mean absolute error (MAE) for the magnitude and distribution of individual errors, as well as the bias error (BE) for the bias of the annual sums.

Method	**R^2_{adj}**	**$RMSE_{abs}$** ($mg\ m^{-2}\ 30min^{-1}$)	**MAE** ($mg\ m^{-2}\ 30min^{-1}$)	**BE** ($g\ m^{-2}\ a^{-1}$)
$MDS_{CO2nofoot}$	0.74	104.35	24.05	13.14
$NLR_{CO2foot}$	0.66	119.10	27.51	-2.12
$NLR_{CH4nofoot}$	0.79	1.36	0.83	-3.34
$NLR_{CH4foot}$	0.81	1.28	0.78	-2.54

942 Table 3: Annual balances of CO_2 and CH_4 derived by different methods for the whole EC source area,
943 the area of interest (AOI) and the two surface types: MDS approach without footprint consideration
944 ($MDS_{CO2nofoot}$), NLR approach without ($NLR_{CH4nofoot}$) and with ($NLR_{CH4foot,}$ $NLR_{CO2foot}$) footprint
945 consideration. Uncertainty was calculated as square root of the sum of squared random uncertainty
946 (measurement uncertainty) and gapfilling uncertainty.

Source area	**Flux** ($g\ m^{-2}\ a^{-1}$)	**Method**			
		CO_2		CH_4	
		$MDS_{CO2nofoot}$	$NLR_{CO2foot}$	$NLR_{CH4nofoot}$	$NLR_{CH4foot}$
Whole EC source area	NEE	524.5 ± 5.6	531.4 ±13.0		
	GPP	-2380.5 ± 5.6	-2122.1 ± 16.7		
	R_{eco}	2863.6 ± 5.6	2603.6 ± 8.4		
	CH_4			40.5 ± 0.2	39.8 ± 0.2
AOI	NEE		843.5 ±13.0		
	GPP		-3192.2 ± 16.7		
	R_{eco}		4035.7 ± 8.4		
	CH_4				21.8 ± 0.2
Emergent vegetation	NEE		750.3 ± 13.0		
	GPP		-4076.8 ± 16.7		
	R_{eco}		4827.2 ± 8.4		
	CH_4				13.2 ± 0.2
Open water	NEE		158.2 ± 13.0		
	GPP		-1021.5 ± 16.7		
	R_{eco}		1179.7 ± 8.4		
	CH_4				52.6 ± 0.2

947

948 Table 4: NEE and net CH_4 exchange at open water sites. The letters in parentheses indicate seasonal
949 (S; May to October) and annual (A) budgets. Positive water level indicates inundated conditions. GHG
950 flux measurement methods are denoted as: CH = chambers, CO = concentration profiles, TR = gas traps.

Reference	**Location, ecosystem type**	**Dominant plant species**	**Study year**	**Average water depth** (m)	**NEE** ($g\ CO_2\ m^{-2}\ a^{-1}$)	**CH_4** ($g\ CH_4\ m^{-2}\ a^{-1}$)
Huttunen et al. (2003), CH	Lake Postilampi, Finland: hypertrophic lake		1997	3.2		16 (A)
Casper et al. (2000), TR/CO	Priest Pot, UK: hypertrophic lake		1997	2.3		13 (A)
Ducharme-Riel et al. (2015), CO	Bran-de-Scie, Quebec: eutrophic lake		2007-2008	3.2	224 (A)	
Wang et al. (2006), CH	Taihu Lake, China, hypertrophic lake:		2003-2004			
	- bare infralittoral zone			0.5 to 1.8		3 (A)
	- pelagic zone			1.8		4 (A)
Hendriks et al. (2007), CH	Horstermeer, The Netherlands: eutrophic ditches		2005	> 0		47 (A)
			2006	> 0		49 (A)
Waddington and Day (2007), CH	Bois-des-Bel peatland, Quebec:		2000-2002			
	- ponds			> 0		0.3 (S)
	- ditches			> 0		2.9 (S)
Naimann et al. (1991), CH	Kabetogama Peninsula, Minnesota, beaver pond:	*Utricularia spp., Potamogeton spp.*	1988			
	- submergent aquatic plants			0.45		14 (A)
	- deep water			1.25		12 (A)
Roulet et al. (1992), CH	Low forest region, Ontario: beaver ponds		1990	0.2 to 0.4		7.6 (A)
Bubier et al. (1993), CH	Clay Belt, Ontario: beaver pond		1991	0.5 to 1.5		44 (A)
Yavitt et al. (1992), CH	New York, beaver ponds:		1990			
	- 3 years old			≤ 2		34 (A)
	- > 30 years old			≤ 2		40 (A)

Table 5: Annual (A)/seasonal (S) NEE, GPP, R_{eco} and net CH_4 exchange at *Typha* sites. Positive water level indicates inundated soil. GHG flux measurement methods are denoted as: CH = chambers, EC = eddy covariance.

Reference	Location, ecosystem type	Dominant plant species	Study year	Mean water level (m)	NEE	GPP ($g\ CO_2\ m^{-2}\ a^{-1}$)	R_{eco}	CH_4 ($g\ CH_4\ m^{-2}\ a^{-1}$)
Kankaala et al. (2004), CH	Lake Vesijärvi, Finland:							
	- inner cattail-reed zone	*Phragmites australis, Typha latifolia*	1997	< 0.1 to > 0.2				51 (S)[1]
			1998	< 0.1 to > 0.2				43 (S)[1], 6 (S)[2]
	- outer cattail-reed zone	*Phragmites australis, Typha latifolia*	1997	< 0.1 to > 0.2				30 (S)[1]
			1998	< 0.1 to > 0.2				23 (S)[1], 7 (S)[2]
			1999	< 0.1 to > 0.2				23 (S)[1]
Chu et al. (2015), EC	Lake Erie, Freshwater marsh	*Typha angustifolia, Nymphaea odorata*	2011	0.3 to 0.6	-289 (A)	-3338 (A)	3049 (A)	58 (A)
			2012	0.3 to 0.6	109 (A)	-3490 (A)	3599 (A)	76 (A)
			2013	0.3 to 0.6	340 (A)	-2666 (A)	3006 (A)	70 (A)
Bonneville et al. (2008), EC Strachan et al. (2015), NEE: EC, CH4: CH	Mer Bleue, Canada, freshwater marsh	*Typha angustifolia*	2005-2006	winter > summer	-967 (A)	-3045 (A)	2078 (A)	
			2005-2009	≈ 0	-462 to - 1041 (A)			170 (A)
Whiting and Chanton (2001), CH	Virginia, freshwater marsh	*Typha latifolia*	1992-1993	0.05 to 0.2	-3288 (A)			109 (A)
	Florida, lake shore	*Typha latifolia*	1992	0.05 to 0.2	-3587 (A)			69 (A)
			1993	0.05 to 0.2	-4177 (A)			96 (A)
Rocha and Goulden (2008), EC	San Joaquin Freshwater Marsh Reserve, California:							
	- freshwater marsh	*Typha latifolia*	1999	winter +, midsummer -		-3994 (A)	4811 (A)	
			2000	winter +, midsummer -	-929 (A)	-6006 (A)		
			2001	winter +, midsummer -	1887 (A)		5980 (A)	
Knox et al. (2015), EC	- wetland (rewetted 2010)	*Schoenoplectus acutus, Typha spp.*	2012	1.07	-1349 (A)	-7717 (A)	6721 (A)	71 (A)
	- wetland (rewetted 1997)	*Schoenoplectus acutus, Typha spp.*	2012	0.26	-1455 (A)	-5519 (A)	4064 (A)	52 (A)
Petrescu et al. (2015), EC	- wetland (rewetted 2010)	?	2010	0.51	388 (A)			21 (A)
Minke et al. (2015), CH	Giel'čykaŭ Kašyl, Belarus, fen (rewetted 1985)	*Typha latifolia, Hydrocharis morsus-ranae*	2010-2011	0.13	553 (A)	-2825 (A)	3375 (A)	80 (A)
			2011-2012	< 0.13	-414 (A)	-3980 (A)	3566 (A)	91 (A)
Günther et al. (2015), CH	Trebeltal, Germany, fen (rewetted 1997)	*Typha latifolia*	2011	0.02	-156 (A)			13 (A)
			2012	-0.09	345 (A)			4 (A)
Wilson et al. (2007, 2008), CH	Turraun, Ireland, cutover bog (rewetted 1991)	*Typha latifolia*	2002	0.07	975 (A)	-3272 (A)	4064 (A)	39 (A)
			2003	0.03	1653 (A)	-4357 (A)	6010 (A)	29 (A)

[1] open water period
[2] winter

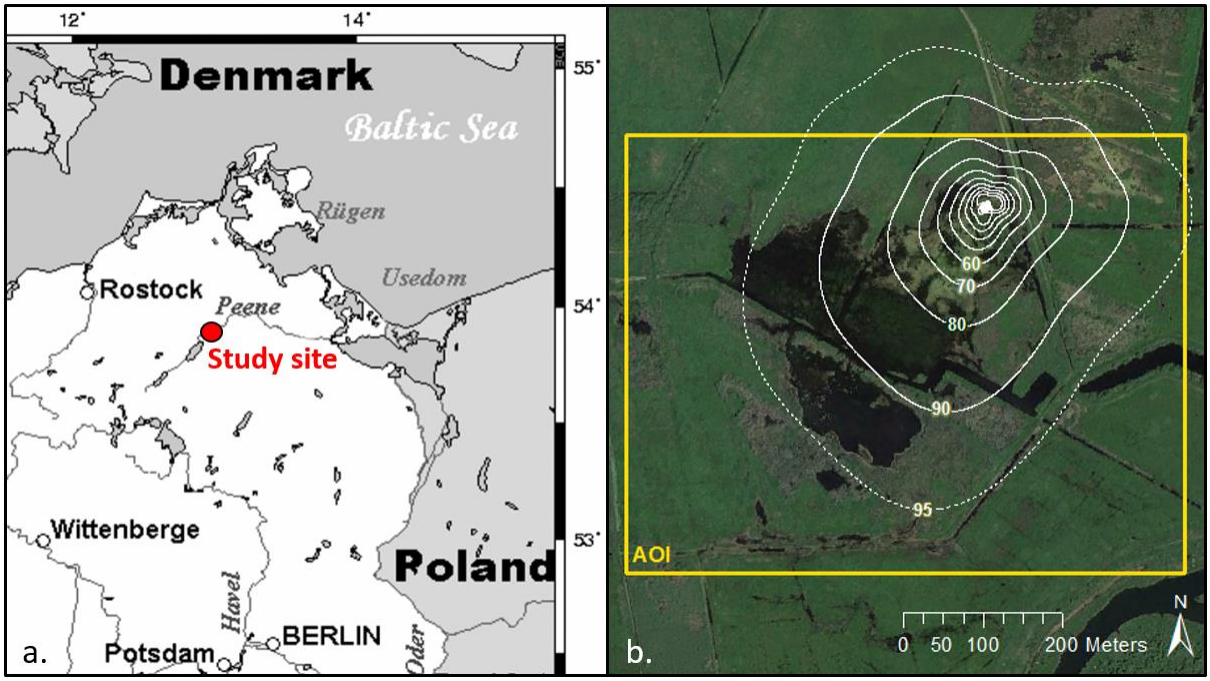

Figure 1: a) Polder Zarnekow is situated in NE Germany within the Peene River valley; map source and copyright: https://commons.wikimedia.org/wiki/File:Germanymap2.png (modified). b) Footprint climatology calculated according to Chen et al. (2011) on a Landsat image (6 Jun 2013, source: Google Earth). White lines represent the isopleths of the cumulative annual footprint climatology, where the area within the 95 isopleth indicates 95 % contribution to the annual flux. The white dot denotes the tower position. The yellow box indicates the area of interest (AOI) as a filter criterion to focus on fluxes of the shallow lake and to avoid the possible impact of a farm and grassland to the north of the shallow lake. If the half-hourly flux source area exceeded the AOI by more than 20 % the flux was discarded. The site is characterised by two main surface types: open water and emergent vegetation.

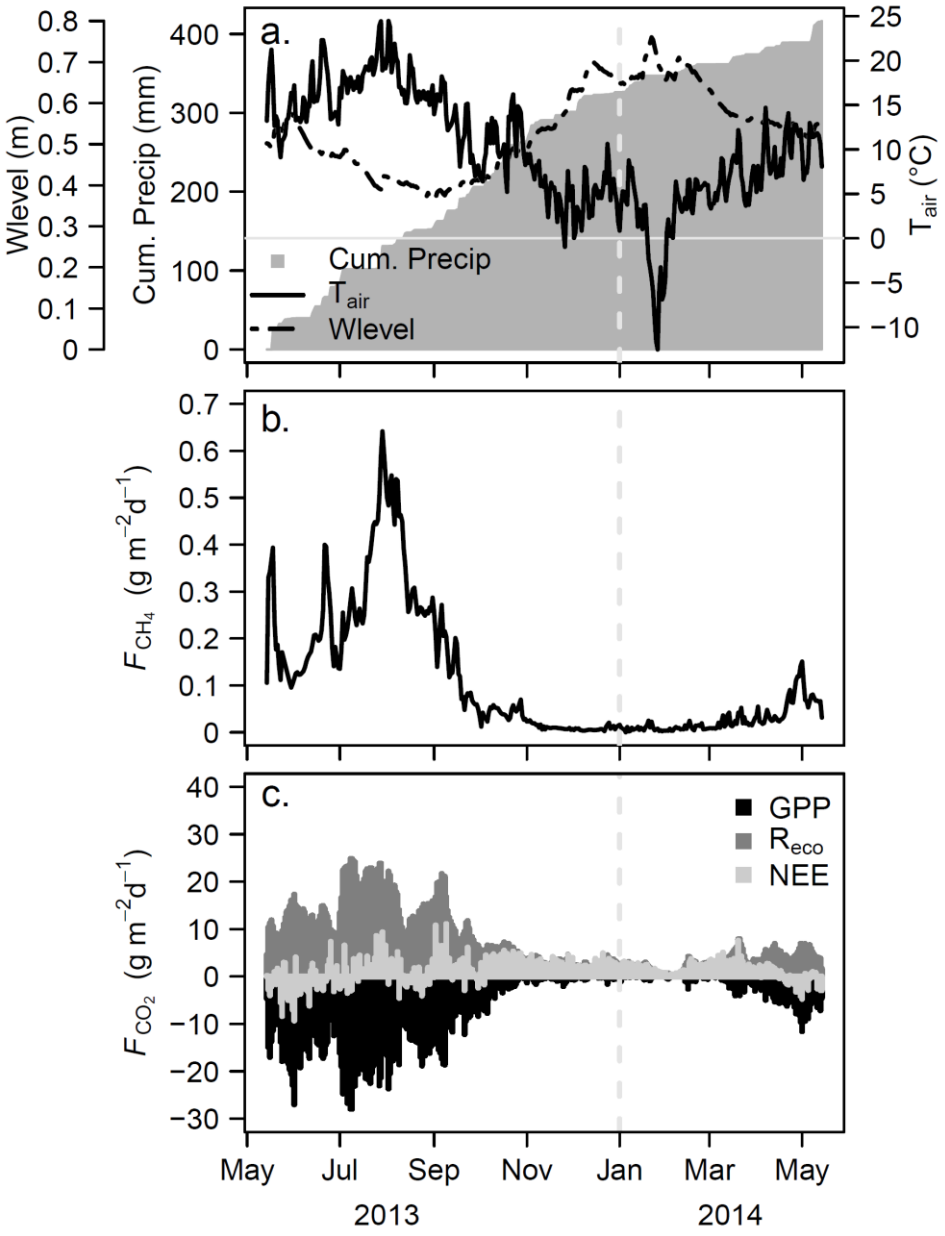

Figure 2: Temporal variability of environmental variables and ecosystem CO_2 and CH_4 exchange within the EC source area. Seasonal course a) of water level (Wlevel), cumulative precipitation (Cum. Precip) and air temperature (T_{air}), b) the daily CH_4 flux (gapfilled, $NLR_{CH4nofoot}$) and c) the daily NEE (gapfilled $MDS_{CO2nofoot}$) and component fluxes (modelled R_{eco} and GPP, $MDS_{CO2nofoot}$).

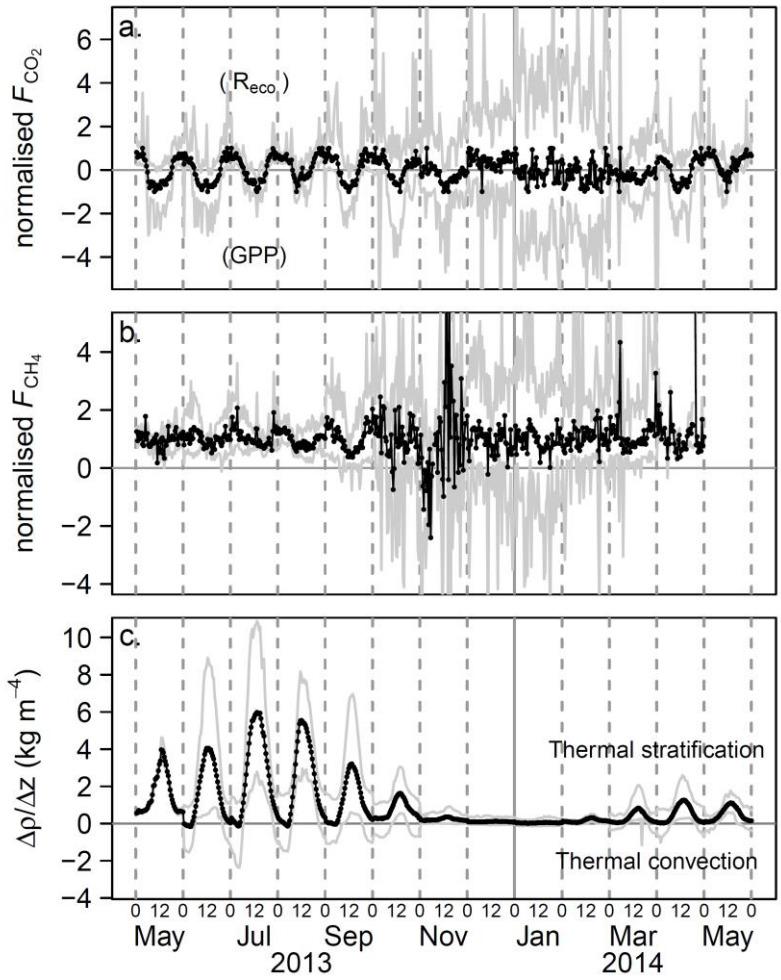

Figure 3: Average diurnal cycle of a) CO_2 flux, b) CH_4 flux and c) the water density gradient per month. The numbers at the x-axis denote midnight (0) and midday (12) in UTC. Midnight is also illustrated with a dashed line. Black and grey lines represent the mean and the range, respectively. The CO_2 and CH_4 fluxes are normalised with the monthly minimum/ maximum and the median of the half-hourly fluxes, respectively. Although the zero line is slightly shifted due to normalisation, positive CO_2 fluxes roughly indicate the dominance of R_{eco} against GPP, negative fluxes the dominance of GPP against R_{eco}. The period of ice-cover was excluded from the calculation of the temperature gradient. A density gradient equal to or below zero indicates thermally induced convective mixing down to the bottom of the open water body of the shallow lake, positive gradients instead thermal stratification.

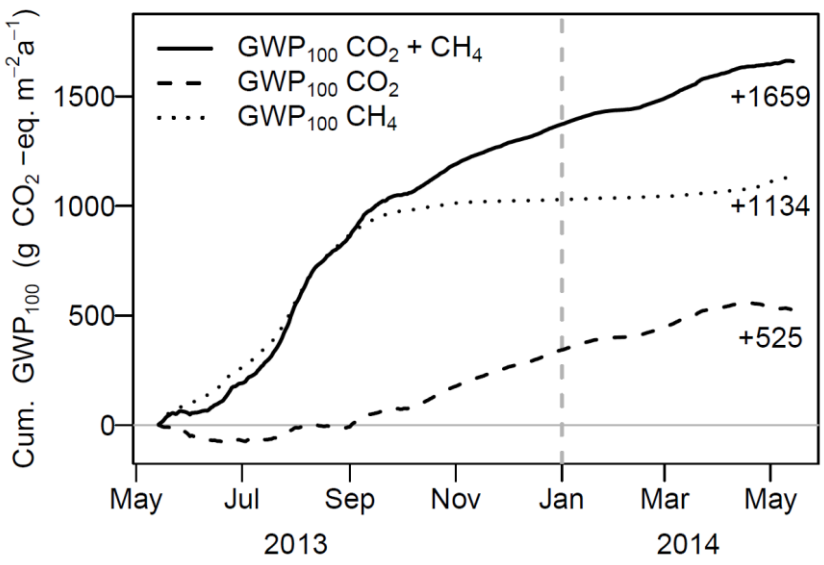

982

983 Figure 4: Cumulative GWP_{100} budgets of CO_2 (based on $MDS_{CO2nofoot}$), CH_4 (based on $NLR_{CH4nofoot}$) and

984 the sum of both for the EC source area during the observation period.

985

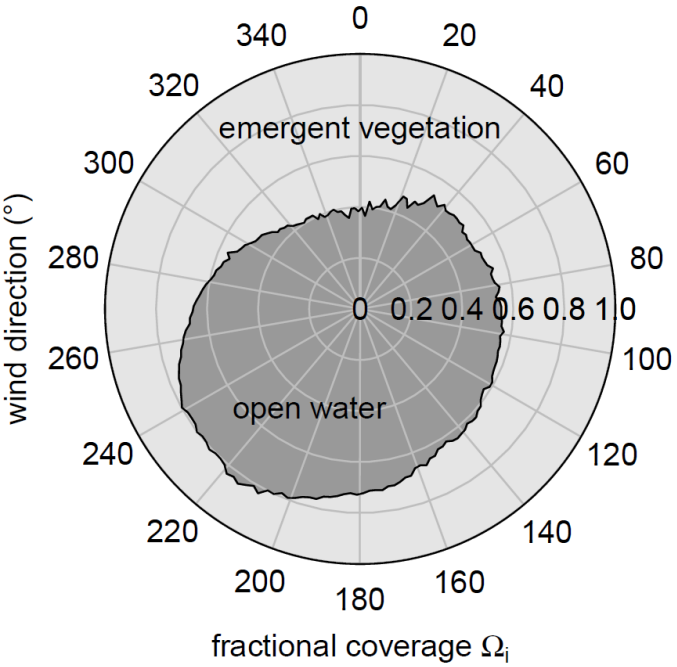

Figure 5: Source area fraction Ω_i of the two main surface types in dependence on the wind direction (2°-bins).

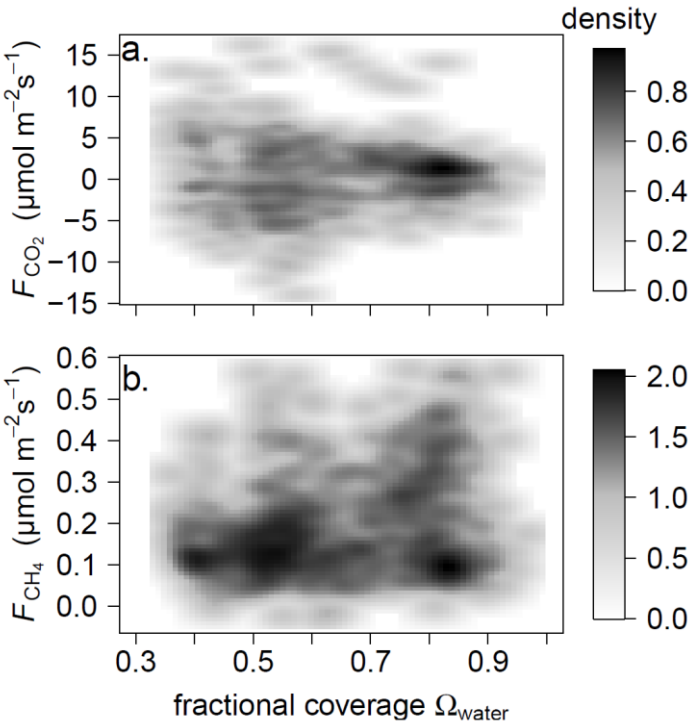

990

991 Figure 6: Impact of the fractional coverage of open water (Ω_{water}) within the EC source area on the
992 measured fluxes of CO_2 and CH_4 (15 May to 14 September 2013). The abundances of CO_2 and CH_4 fluxes
993 in dependence on Ω_{water} are illustrated by a smoothed two-dimensional kernel density estimate. The
994 variability of CO_2 flux rates decreased with increasing Ω_{water}, whereas the variability of the CH_4 flux
995 increased.

996

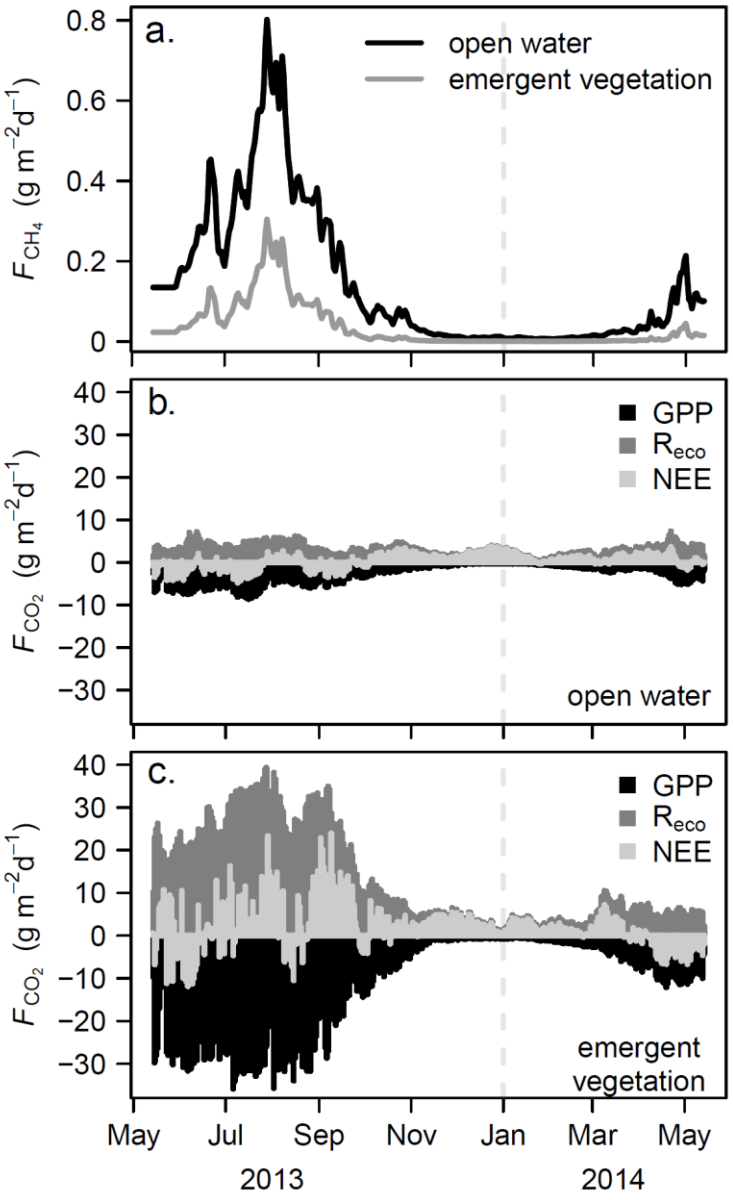

997

998 Figure 7: Daily CH_4, NEE and component fluxes (R_{eco} and GPP) for the surface types: a) daily CH_4 flux of
999 open water and emergent vegetation, b) daily NEE and component fluxes for open water, c) daily NEE
1000 and component fluxes for emergent vegetation, derived by NLR with the source area fractions of the
1001 surface types (Ω_i) as weighting factors ($NLR_{CH4foot}$, $NLR_{CO2foot}$).

1002

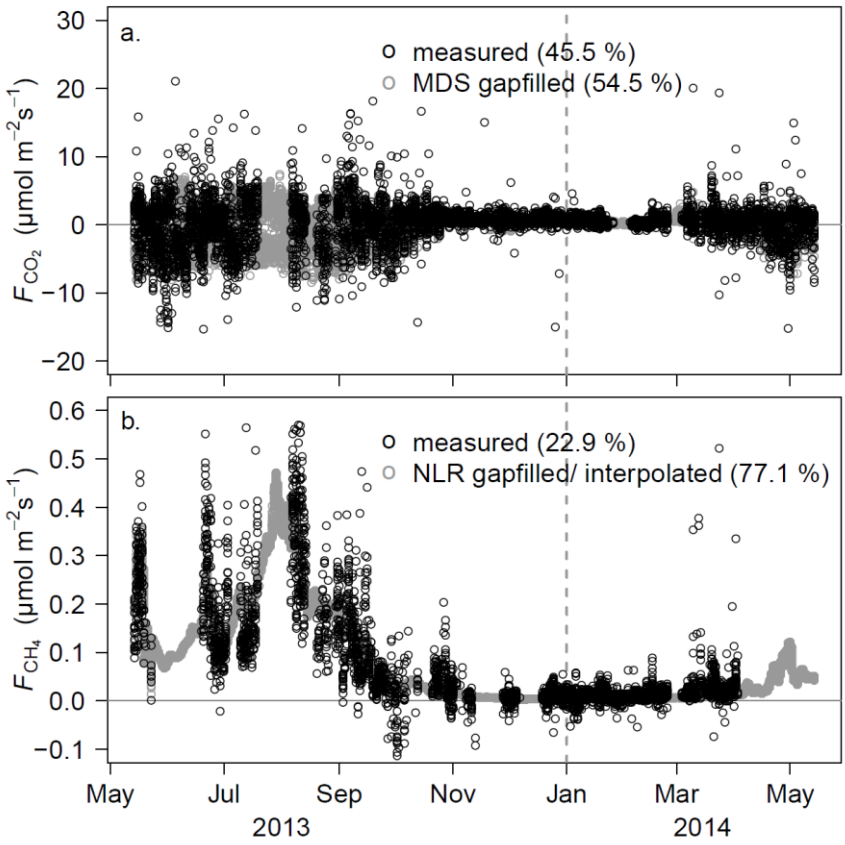

Figure A1: Data coverage of a) CO_2 and b) CH_4 fluxes within the study period. Gapfilling results of the $MDS_{CO2nofoot}$ and $NLR_{CH4nofoot}$ approaches are added as grey circles. The percentages in brackets indicate the time series coverages of measurements and gapfilling values.